

OAK RIDGE NATIONAL LABORATORY

OPERATED BY  
UNION CARBIDE CORPORATION  
NUCLEAR DIVISION



POST OFFICE BOX X  
OAK RIDGE, TENNESSEE 37830

NOTICE  
This report was prepared as an account of work sponsored by the United States Government. Neither the United States nor the United States Energy Research and Development Administration, nor any of their employees, nor any of their contractors, subcontractors, or their employees, makes any warranty, express or implied, or assumes any legal liability or responsibility for the accuracy, completeness or usefulness of any information, apparatus, product or process disclosed, or represents that its use would not infringe privately owned rights.

ORNL/MIT-219

DATE: November 21, 1975

COPY NO.

SUBJECT: Determination and Correlation of Hydrodynamic Variables in a Three-Phase Fluidized Bed

Authors: S.R. Bloxom, J.M. Costa, J. Herranz, S.R. Roth, and G.L. MacWilliam

Consultants: J.M. Begovich and J.S. Watson

#### ABSTRACT

The basic hydrodynamic variables of minimum fluidization velocity and phase holdups were experimentally measured in a three-phase fluidized bed utilizing a pressure profile technique. The effect of the liquid viscosity on the hydrodynamic variables was determined with glycerine-water solutions ranging in viscosity from 0.9 to 11.5 cp. Computerized techniques for data handling and analysis are presented. Correlations for the phase holdups and minimum fluidization velocities as functions of the phase properties and operating parameters are presented for the experimental data and for data compiled from literature sources. An error analysis was performed on the experimental procedure to identify specific procedures requiring modification or control.

M.I.T. Station  
School of Chemical Engineering Practice  
Massachusetts Institute of Technology

MASTER

DISTRIBUTION OF THIS DOCUMENT IS UNLIMITED  
CONTRACT NO. W-7405-ENG-26

## **DISCLAIMER**

**This report was prepared as an account of work sponsored by an agency of the United States Government. Neither the United States Government nor any agency thereof, nor any of their employees, makes any warranty, express or implied, or assumes any legal liability or responsibility for the accuracy, completeness, or usefulness of any information, apparatus, product, or process disclosed, or represents that its use would not infringe privately owned rights. Reference herein to any specific commercial product, process, or service by trade name, trademark, manufacturer, or otherwise does not necessarily constitute or imply its endorsement, recommendation, or favoring by the United States Government or any agency thereof. The views and opinions of authors expressed herein do not necessarily state or reflect those of the United States Government or any agency thereof.**

## **DISCLAIMER**

**Portions of this document may be illegible in electronic image products. Images are produced from the best available original document.**

Printed in the United States of America. Available from  
National Technical Information Service  
U.S. Department of Commerce  
5285 Port Royal Road, Springfield, Virginia 22161  
Price: Printed Copy \$5.00; Microfiche \$2.25

This report was prepared as an account of work sponsored by the United States Government. Neither the United States nor the Energy Research and Development Administration/United States Nuclear Regulatory Commission, nor any of their employees, nor any of their contractors, subcontractors, or their employees, makes any warranty, express or implied, or assumes any legal liability or responsibility for the accuracy, completeness or usefulness of any information, apparatus, product or process disclosed, or represents that its use would not infringe privately owned rights.



## Contents

	<u>Page</u>
1. Summary .....	4
2. Introduction .....	5
2.1 Background .....	5
2.2 Previous Work .....	6
2.3 Objectives and Method of Attack .....	6
3. Apparatus and Procedure .....	7
3.1 Apparatus .....	7
3.2 Procedure .....	7
4. Results and Discussion of Results .....	9
4.1 Fluid Effects on the Hydrodynamic Variables .....	9
4.1.1 Bed Pressure Drop .....	9
4.1.2 Minimum Fluidization Velocity .....	14
4.1.3 Phase Holdups .....	14
4.2 Error Analysis .....	14
4.3 Correlation of Hydrodynamic Variables .....	26
4.3.1 Approach .....	26
4.3.2 Solid Holdup .....	27
4.3.3 Gas Holdup .....	30
4.3.4 Liquid Holdup .....	30
4.3.5 Minimum Fluidization Velocity .....	36
5. Conclusions .....	36
6. Recommendations .....	37
7. Acknowledgment .....	38
8. Appendix .....	39
8.1 Error Analysis Calculations .....	39
8.2 Computerized Data Analysis .....	41
8.3 Correlation Program .....	59
8.4 Location of Data .....	70
8.5 Nomenclature .....	70
8.6 Literature References .....	71

## 1. SUMMARY

To evaluate the effect of liquid viscosity on three-phase fluidization, 5-mm glass beads were fluidized with various water-glycerine solutions ranging in viscosity from 0.9 to 11.5 cp. All three phase holdups and minimum fluidization velocities were measured using a bed pressure profile technique. A computer program for the data processing required by this technique was developed, enabling rapid and consistent analysis of the experimental data.

An error analysis was performed on the experimental procedure to identify those steps requiring modification or control. The absolute error associated with the calculation of each phase holdup was essentially constant over a wide range of operating conditions. The major sources of experimental error were in the measurement of the solid density and the determination of the bed height and pressure drop. The absolute error resulting from these measurements was most significant for the gas and liquid holdups.

Correlations for the phase holdups and minimum fluidization velocities were determined from both the experimental data and from data reported in the literature. Two different correlations were found for the solid phase holdup depending on which data were correlated. For the ORNL data, which includes the experimental data from this investigation and the data obtained by Khosrowshahi *et al.* (8), the solid phase holdup could be represented by:

$$1 - \epsilon_S = 1.03 Fr_L^{0.094 \pm 0.003} Ga^{-0.026 \pm 0.001} \quad (1)$$

On expanding the data base to include that reported in the literature by a variety of authors (1, 2, 4, 6, 9, 11, 12, 13), a different correlation for the solid holdup was determined:

$$1 - \epsilon_S = 1.53 Re_L^{0.275 \pm 0.005} Ga^{-0.171 \pm 0.003} \quad (2)$$

The gas holdup depended predominantly on the gas velocity and was only slightly dependent on the liquid velocity and independent of the liquid viscosity. The correlation determined for the prediction of the gas holdup was

$$\epsilon_G = 0.15 \left( \frac{U_G^5 \rho_L}{U_L^6 \sigma_L g} \right)^{0.100 \pm 0.003} \quad (3)$$

This correlation was based only on the experimental data measured in this investigation, since sufficient reliable data for gas holdup could not be found in the literature.

A dimensional correlation for the liquid phase holdup was obtained:

$$\varepsilon_L = 0.45 U_L^{0.269 \pm 0.007} U_G^{-0.146 \pm 0.010} (\rho_S - \rho_L)^{-1.072 \pm 0.034} \quad (4)$$

Similarly, the liquid minimum fluidization velocity was correlated as functions of the dimensional operating parameters:

$$U_{L_{mf}} = 0.014 \rho_S^{3.70 \pm 0.153} \mu^{-0.473 \pm 0.015} \quad (5)$$

This correlation was based on a restricted operating range, however. A dimensionless correlation for either the liquid holdup or minimum fluidization velocity could not be obtained.

Recommendations for the future investigation of three-phase fluidized beds were presented. Variation of alternative operating parameters was suggested as necessary for verification of the obtained correlations and for identification of other operating dependencies. Further correlations, particularly of a non-product form, should be attempted to allow for more accurate prediction of the hydrodynamic variables. Improvements were proposed in the experimental procedure and techniques.

## 2. INTRODUCTION

### 2.1 Background

In three-phase fluidization a bed of solid particles is suspended by an upward cocurrent flow of both gas and liquid. The principal application of this technique is as a contactor for catalytic reactions involving gas and liquid reactants and a solid catalyst. Current industrial processes utilizing this technique include catalytic hydrogenation of petroleum stocks, coal liquefaction, and biochemical conversions. A better understanding of the flow behavior in a three-phase fluidized bed is essential for the design analysis of such industrial operations. However, current theoretical models are unsuccessful in adequately describing the hydrodynamics of a three-phase fluidized bed, and empirically derived correlations are often contradictory among investigators. To obtain a general correlation describing the behavior of a three-phase fluidized system, it is necessary to compile and analyze data over a wide range of operating conditions.

## 2.2 Previous Work

The solid holdup in a three-phase fluidized bed has been measured by a number of investigators over a wide range of operating conditions and a variety of correlating parameters have been presented in describing the flow behavior of the fluidized system. Several authors (1, 5, 13) have attempted correlations based on a generalized bubble wake model. Others have presented correlations for the phase holdups in terms of both dimensional and non-dimensional groups (3, 4, 7, 8, 9, 12). To obtain a reliable correlation, it is necessary to cover a wide range of operating conditions. In an extensive study of three-phase fluidization, Kim *et al.* (9) demonstrated the importance of viscosity on the phase holdups, an effect not considered in the predominantly air-water-solid fluidization studies of other investigators. In the most recent study on three-phase fluidization, Khowrowshahi *et al.* (8), recognizing the importance of considering a wide range of operating conditions, collected and compiled information from a number of authors (4, 6, 9, 12) in his study of the hydrodynamic variables in a three-phase fluidized bed.

## 2.3 Objectives and Method of Attack

To evaluate the effect of viscosity on three-phase fluidization, 5-mm glass particles were fluidized with air and five different water-glycerine solutions ranging from 0 to 66% glycerine by weight. The phase holdups of this system were determined from Eqs. (6), (7), and (8).

$$\epsilon_S = M_S / \rho_S A H_B \quad (6)$$

$$\Delta P = (\epsilon_S \rho_S + \epsilon_L \rho_L + \epsilon_G \rho_G) g H_B \quad (7)$$

$$1 = \epsilon_S + \epsilon_L + \epsilon_G \quad (8)$$

The bed height, pressure drop across the bed, and minimum fluidization velocities were obtained by the longitudinal pressure profile technique previously employed by other investigators (1, 8, 9, 11). The laborious manual plotting and graphical analysis required by this technique has been incorporated into a computer program enabling rapid and consistent analysis of the experimental data.

The experimental data were correlated both independently and in conjunction with data compiled from the literature (1, 2, 11, 13). The correlation procedure involved a step-wise multiple linear regression for dimensional, and subsequently, significant non-dimensional operating parameters. A product form of correlation in terms of the dimensional operating parameters

was first assumed. The variables of lesser importance, based on a t-test, were successively eliminated until further reduction in the number of variables significantly reduced the correlation coefficient. Product forms of the dimensionless groups formed from the significant dimensional variables were then correlated with the best correlation being found by a modified step-wise process. This procedure identified the significant operating variables and eliminated conflicting interactions of the dimensionless groups.

An error analysis was performed on the experimental procedure to identify the specific procedures requiring modification or control. The error analysis for the phase holdups was performed using second power equations for single sample experiments following a technique outlined by Kline and McClintock (10). The specific set of operating conditions analyzed were selected based on the bounding values of the experimental operating conditions.

### 3. APPARATUS AND PROCEDURE

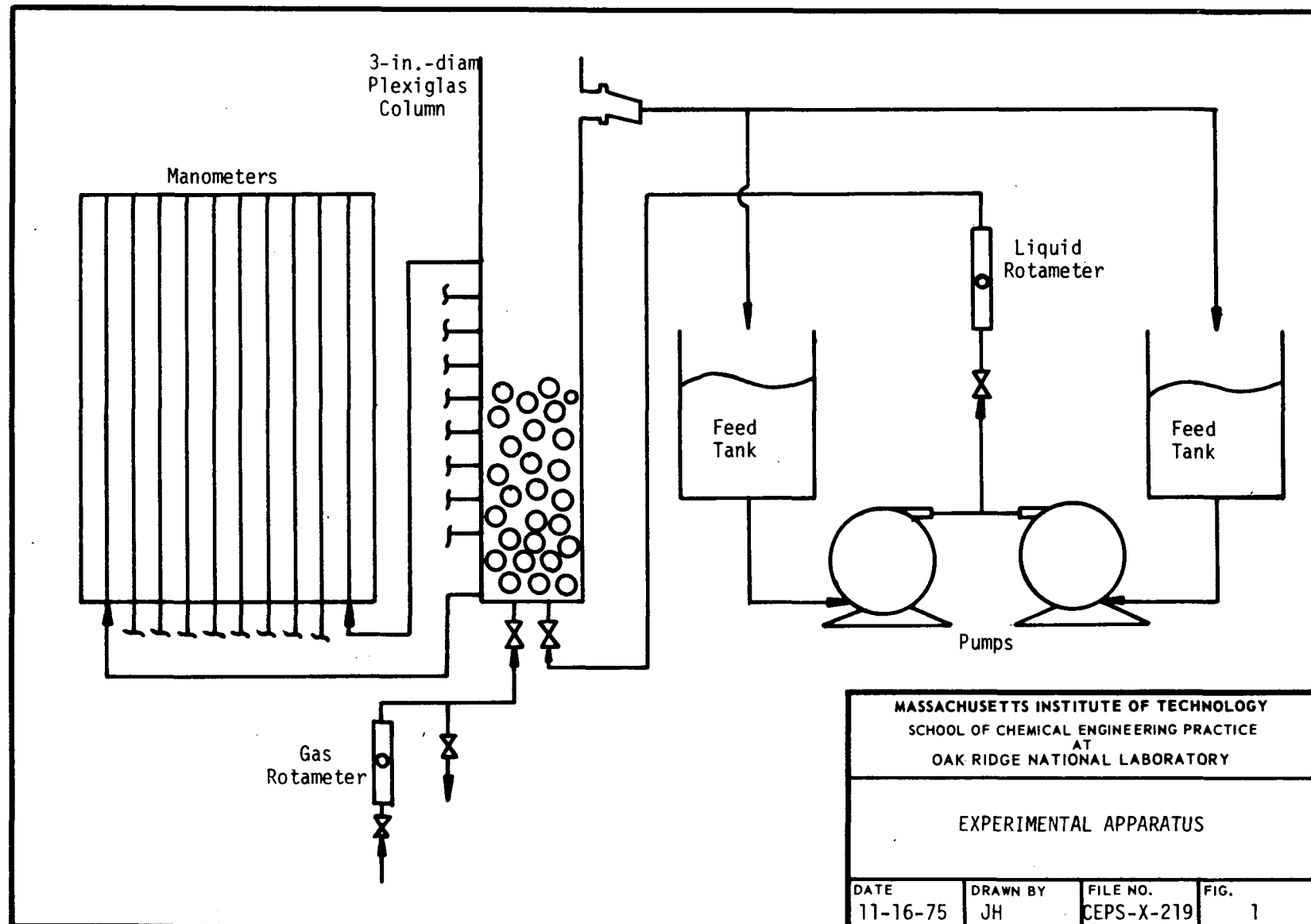
#### 3.1 Apparatus

The experimentation was conducted in the apparatus shown in Fig. 1. Liquid was pumped from the 55-gal feed tanks through a series of rotameters to the bottom of a 3-in.-diam Plexiglas column where a 50-mesh screen acted as a liquid distributor. Similarly, air flowed from an air line through a series of gas rotameters and entered the column through a cross-shaped gas distributor located directly above the liquid distributor. The gas and liquid flowed cocurrently upwards through the column, the exit air being vented to atmosphere and the liquid recycled to the feed tanks. A series of manometers located at intervals along the column wall enabled measurement of the pressure profile up the column.

#### 3.2 Procedure

The Plexiglas column was charged with 2500 gm of 0.462-cm-diam glass beads, the beads having an average density of 2.26 gm/cm<sup>3</sup>. These particles were fluidized by both air and a water-glycerine solution, the solution ranging from 0-66% glycerine by weight (0.9-11.5 cp). The densities of all liquid solutions were determined using a calibrated hydrometer and the viscosities measured with a Fenske tube viscometer. The viscosity was checked frequently to detect variations due to temperature and water evaporation.

For each of the five water-glycerine solutions, fluidization studies were conducted at five superficial gas velocities ranging from 3.5 to 14.0 cm/sec. At every gas velocity, the superficial liquid velocity was varied from 1.0 to 8.3 cm/sec. The pressure profile up the column was measured



at each liquid velocity by the series of manometers along the column. The pressure drop due to flow at any position in the column was calculated as the difference between the height of fluid in the manometer located at that position and the height in the bottom manometer. The solids bed height and pressure drop across the bed were determined by a plot of pressure drop against distance up the column as shown in Fig. 2. Here the point of intersection of the two straight lines represents a change in the pressure gradient up the column and the transition from the three phase region to the two-phase bubble column region above the bed. The bed height and pressure drop obtained in this manner were substituted into Eqs. (6), (7), and (8) to calculate the phase holdups. A series of such measurements were made at several different liquid flow rates for a constant gas flow rate. The minimum fluidization velocities were determined, as shown in Fig. 3, by a plot of the pressure drop against the superficial liquid velocity. All calculations, plotting, and data analyses were performed by the computer programs documented in Appendix 8.2.

#### 4. RESULTS AND DISCUSSION OF RESULTS

##### 4.1 Fluid Effects on the Hydrodynamic Variables

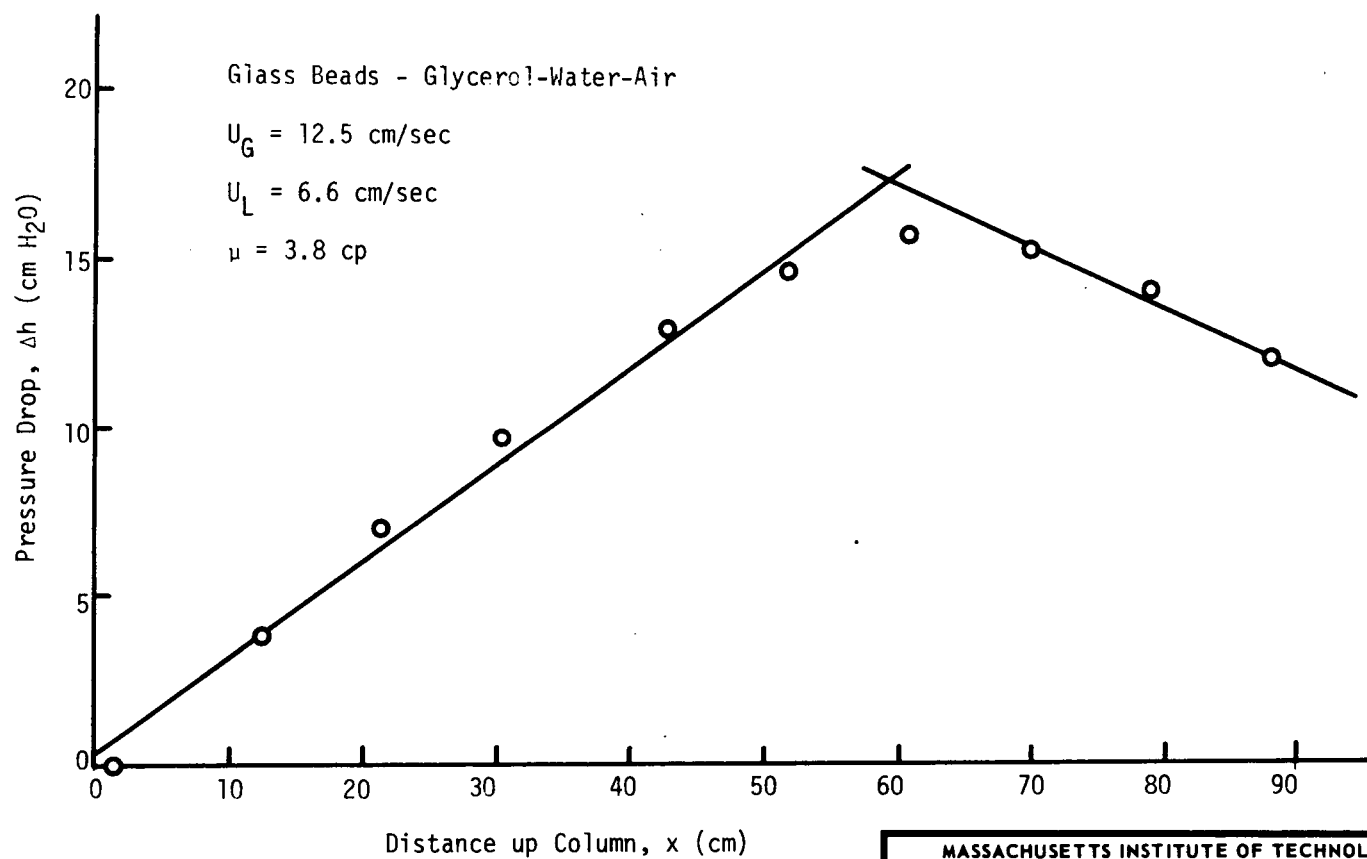
###### 4.1.1 Bed Pressure Drop

The reduced pressure drop through the solid bed as a function of the superficial liquid velocity is shown in Fig. 4 for three gas velocities at a constant liquid viscosity. This pressure drop is based on the buoyant weight of the solid bed:

$$w_{buoy} = M_S \left( \frac{\rho_S - \rho_f}{\rho_S} \right) g \quad (9)$$

The pressure drop increased with increasing liquid velocities prior to fluidization. The minimum liquid fluidization velocity was determined at the point at which the pressure drop became independent of further increases in liquid velocity. For the water-air fluidization system depicted in Fig. 4, the maximum bed pressure drop and the minimum liquid fluidization velocity decreased with increases in the gas superficial velocity.

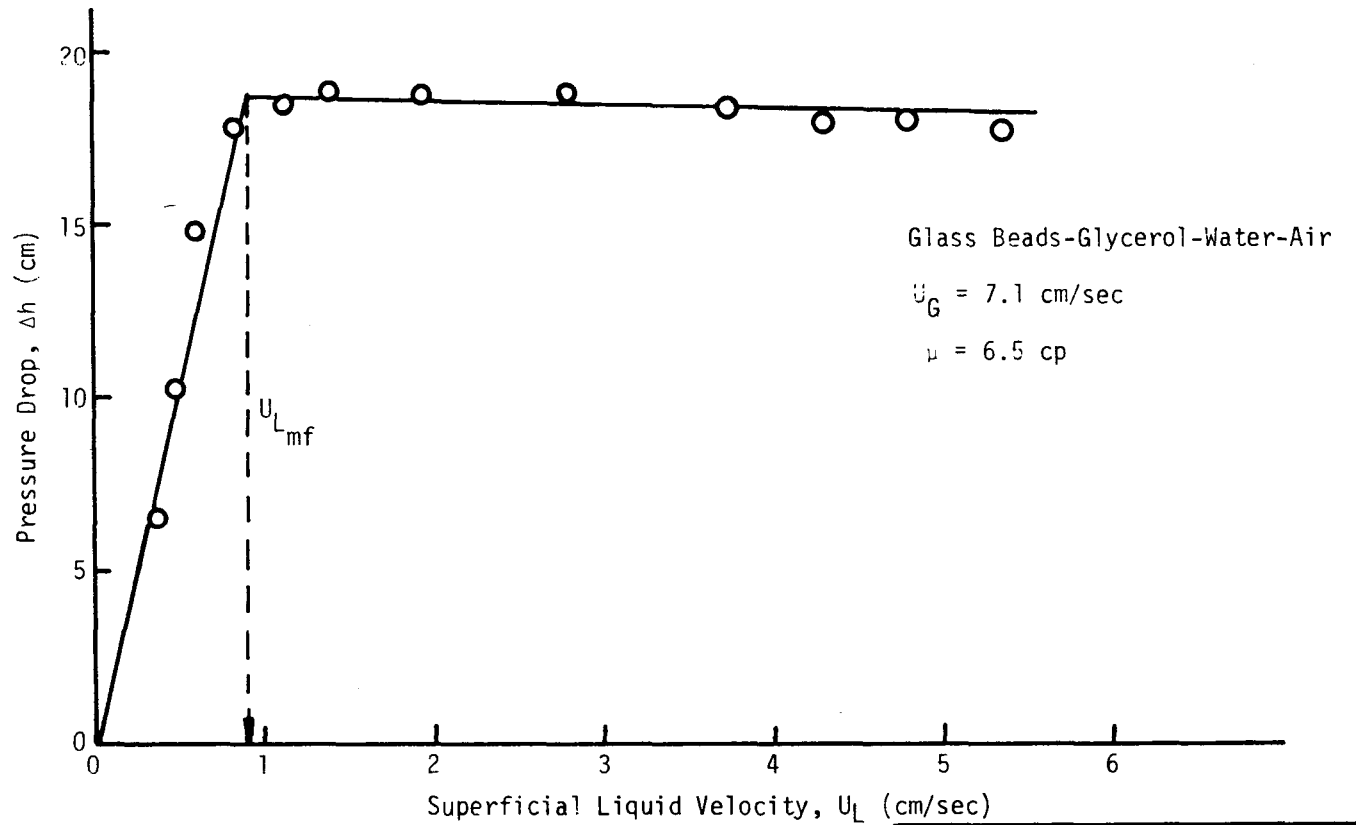
In Fig. 5 the reduced pressure drop through the bed as a function of the superficial liquid velocity is shown for three different liquid viscosities at a constant gas velocity. Again, the pressure drop increased with increasing liquid velocity below minimum fluidization. With increasing liquid viscosity, the maximum bed pressure drop and the minimum liquid fluidization velocity were lowered. This is the result of the larger upward drag force exerted on the solid particles by the higher viscosity solutions.



MASSACHUSETTS INSTITUTE OF TECHNOLOGY  
SCHOOL OF CHEMICAL ENGINEERING PRACTICE  
AT  
OAK RIDGE NATIONAL LABORATORY

DETERMINATION OF BED HEIGHT

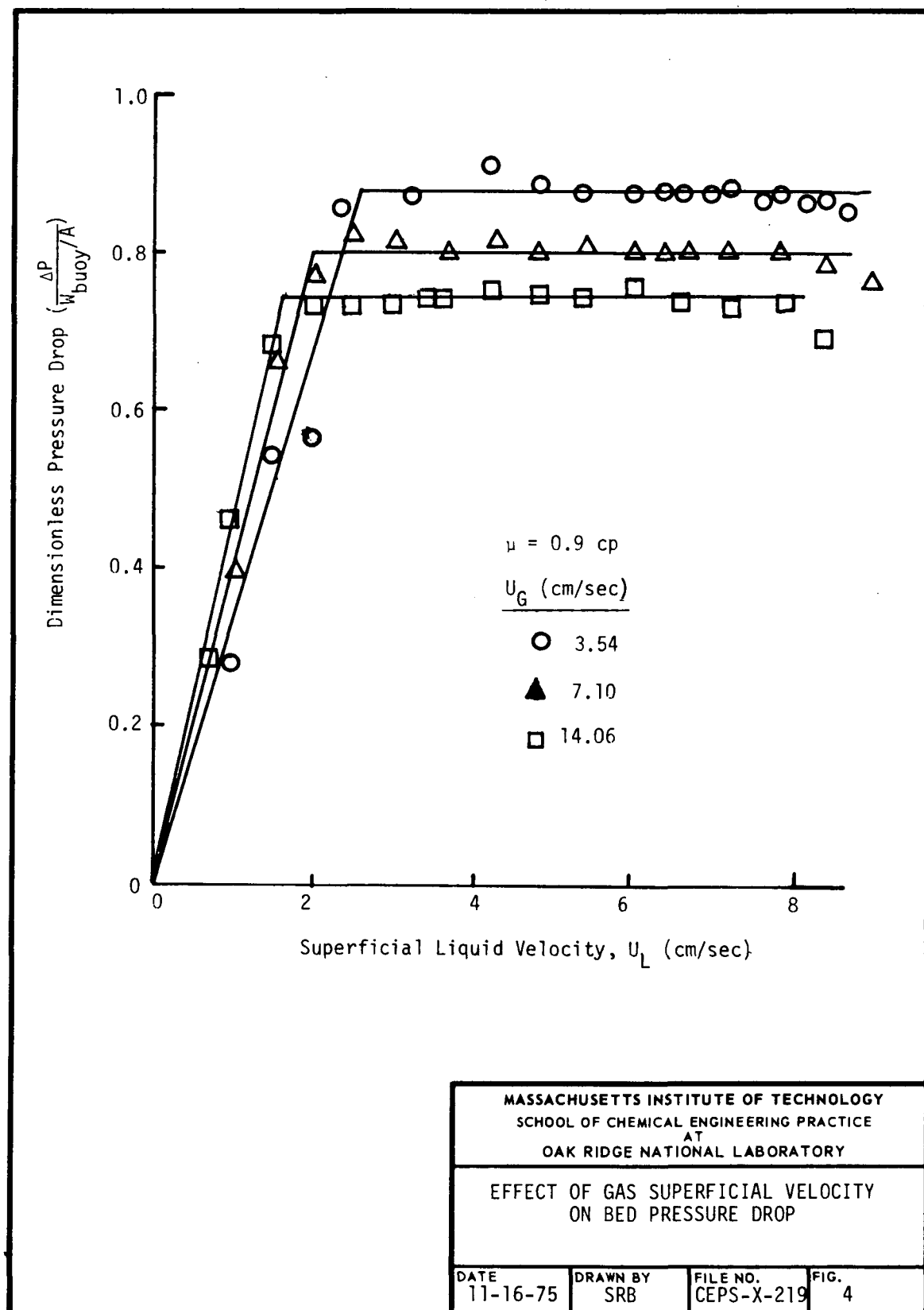
DATE 11-16-75	DRAWN BY JH	FILE NO. CEPS-X-219	FIG. 2
------------------	----------------	------------------------	-----------

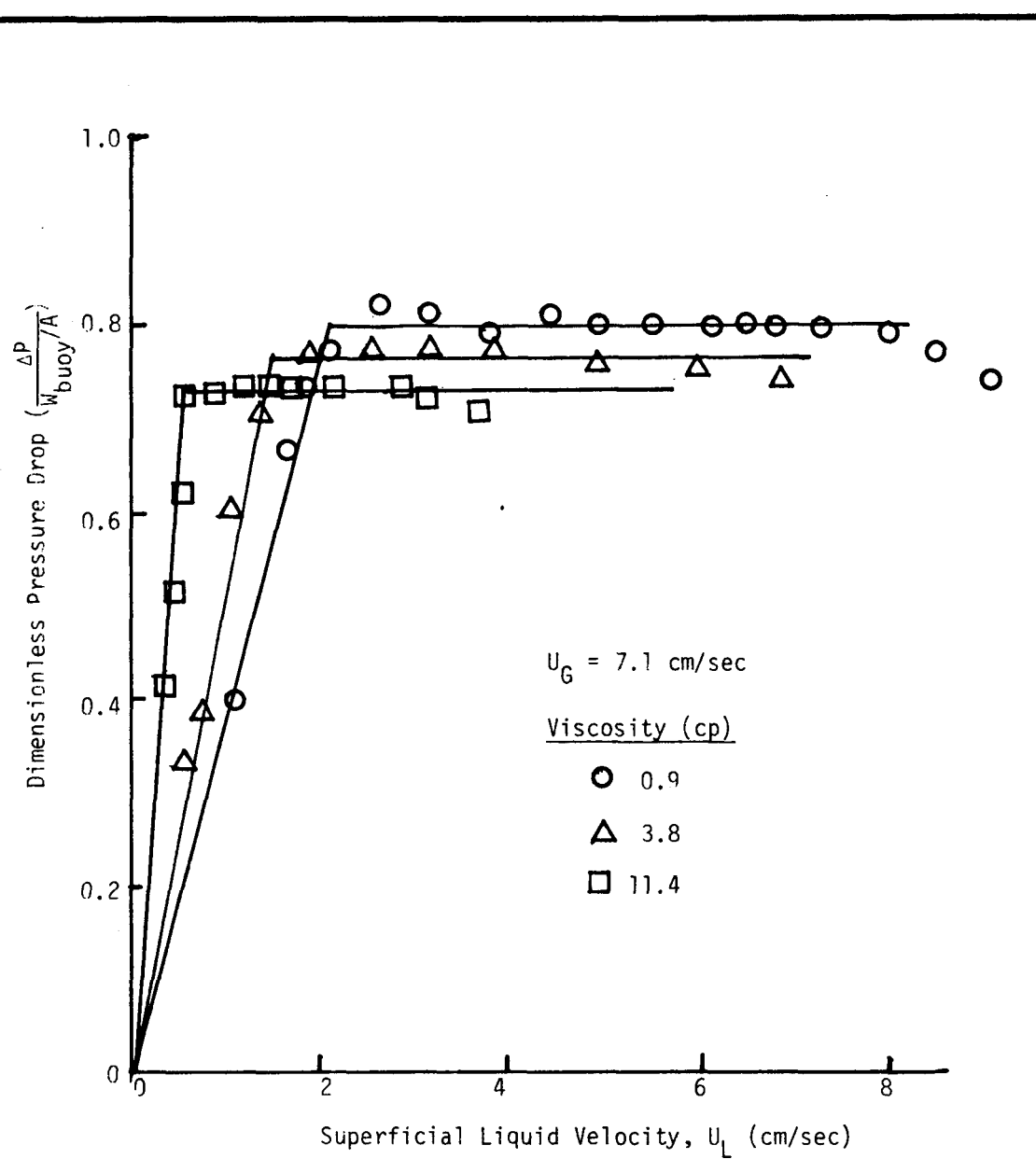


MASSACHUSETTS INSTITUTE OF TECHNOLOGY  
SCHOOL OF CHEMICAL ENGINEERING PRACTICE  
AT  
OAK RIDGE NATIONAL LABORATORY

DETERMINATION OF MINIMUM  
FLUIDIZATION VELOCITY

DATE 11-16-75	DRAWN BY JH	FILE NO. CEPS-X-219	FIG. 3
------------------	----------------	------------------------	-----------





MASSACHUSETTS INSTITUTE OF TECHNOLOGY  
SCHOOL OF CHEMICAL ENGINEERING PRACTICE  
AT  
OAK RIDGE NATIONAL LABORATORY

EFFECT OF VISCOSITY ON  
BED PRESSURE DROP

DATE 11-16-75	DRAWN BY SRB	FILE NO. CEPS-X-219	FIG. 5
------------------	-----------------	------------------------	-----------

#### 4.1.2 Minimum Fluidization Velocity

The effect of liquid viscosity on the minimum fluidization velocities is illustrated in Fig. 6. The points on the ordinate correspond to the theoretical values for the liquid minimum fluidization velocity in a two-phase fluidized bed. These values were calculated from the correlation derived by Wen and Yu (15):

$$Re_{mf} = [(33.7)^2 + 0.0408 Ar]^{1/2} - 33.7 \quad (10)$$

It is apparent from Fig. 6 that for a given superficial gas velocity, the minimum liquid fluidization velocity decreases as the liquid viscosity is increased. For the range of operating conditions studied, the minimum liquid fluidization velocity was independent of the gas velocity for the more viscous solutions. The extrapolation of the minimum fluidization velocities to the two-phase region does indicate some dependence on the gas velocity. However, the form of this dependence cannot be evaluated due to the restricted range of operations.

#### 4.1.3 Phase Holdups

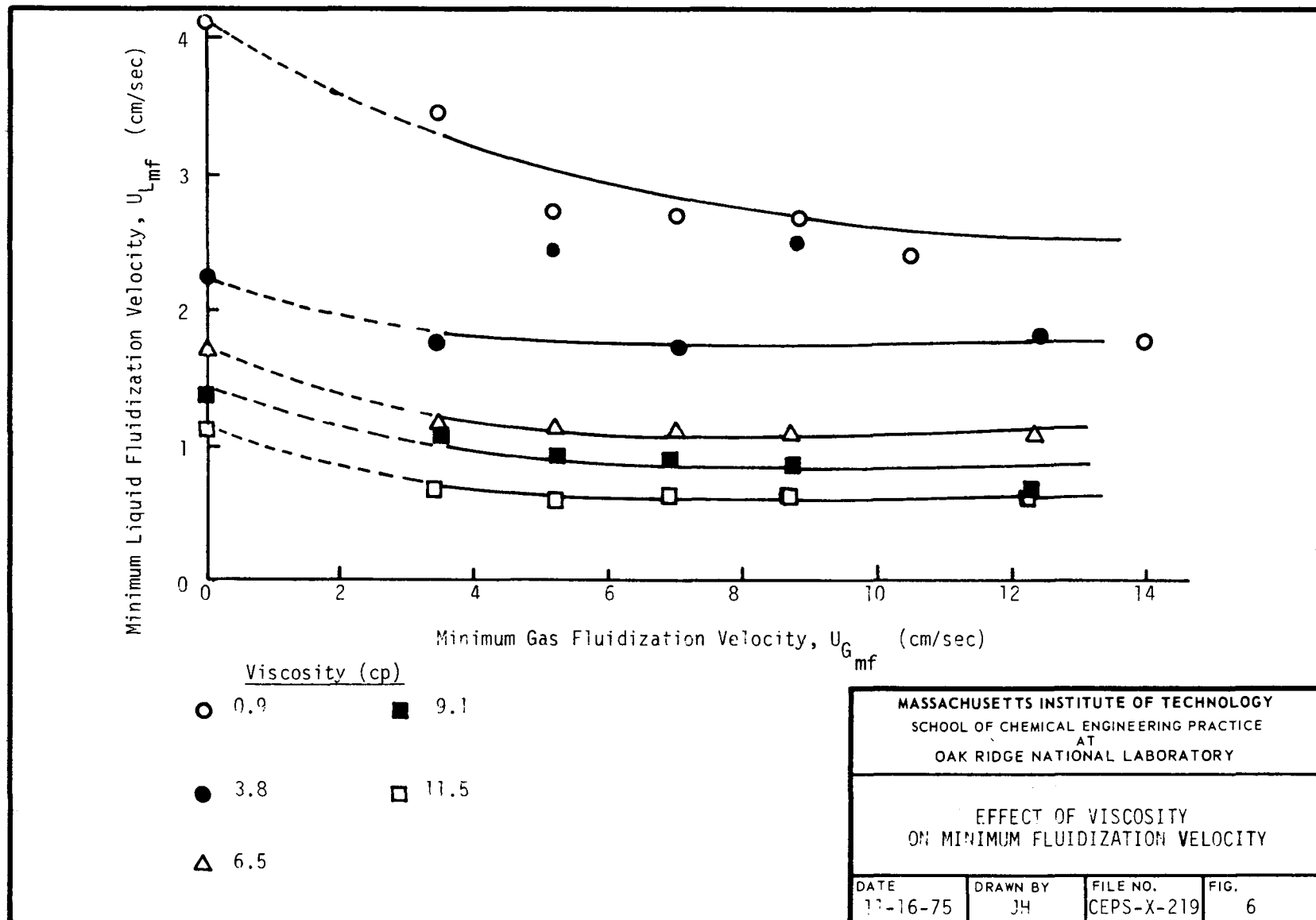
The effect of the liquid and gas superficial velocities on the solid, liquid, and gas holdups are shown in Figs. 7 through 10. The larger drag forces applied to the solid particles by an increase in the liquid velocity causes the solid bed to expand. This results in a significant decrease in the solid holdup and a counterbalancing increase in the liquid holdup with only a slight effect on the gas holdup as shown in Fig. 7.

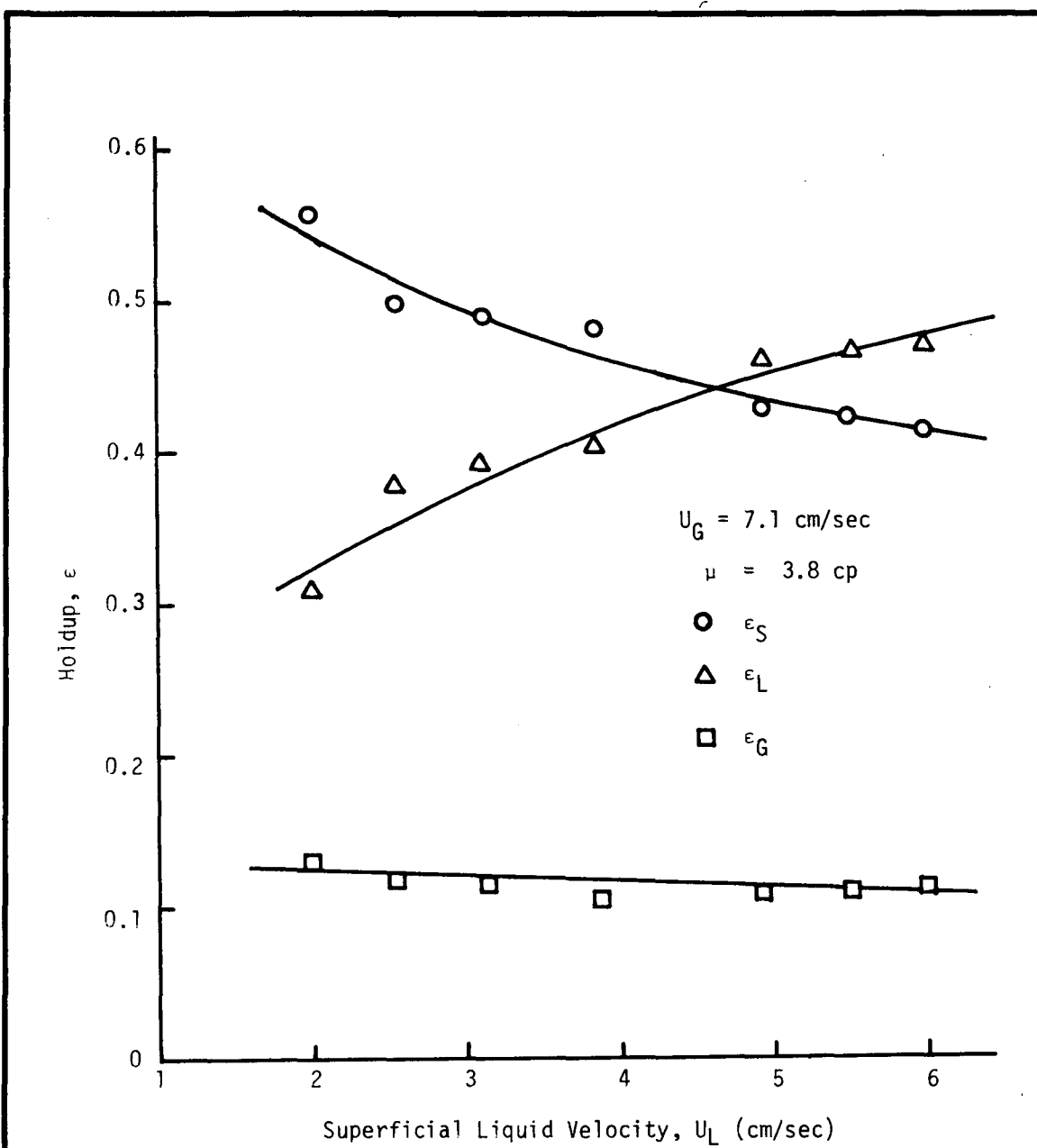
A variation in the gas velocity affects primarily the gas and liquid holdup with little change in the solid holdup. The result of changing the superficial gas velocity on the phase holdups is illustrated in Figs. 8 through 10.

The effect of the liquid viscosity on the different phase holdups is shown in Figs. 11 through 14. A higher solution viscosity yields higher drag forces on the solid particles at constant fluid velocities. The result of increasing the liquid viscosity is similar to increasing the liquid velocity. The solid holdup decreases with a compensating increase in the liquid holdup as shown in Figs. 11 and 12. The liquid viscosity does not affect the gas holdup as shown on Fig. 13. The effect of the viscosity on the bed porosity shown in Fig. 14 is comparable to the effect demonstrated by Kim *et al.* (9).

## 4.2 Error Analysis

In most engineering experiments it is not practical to estimate all of the uncertainties of observations by repetition; a single observation

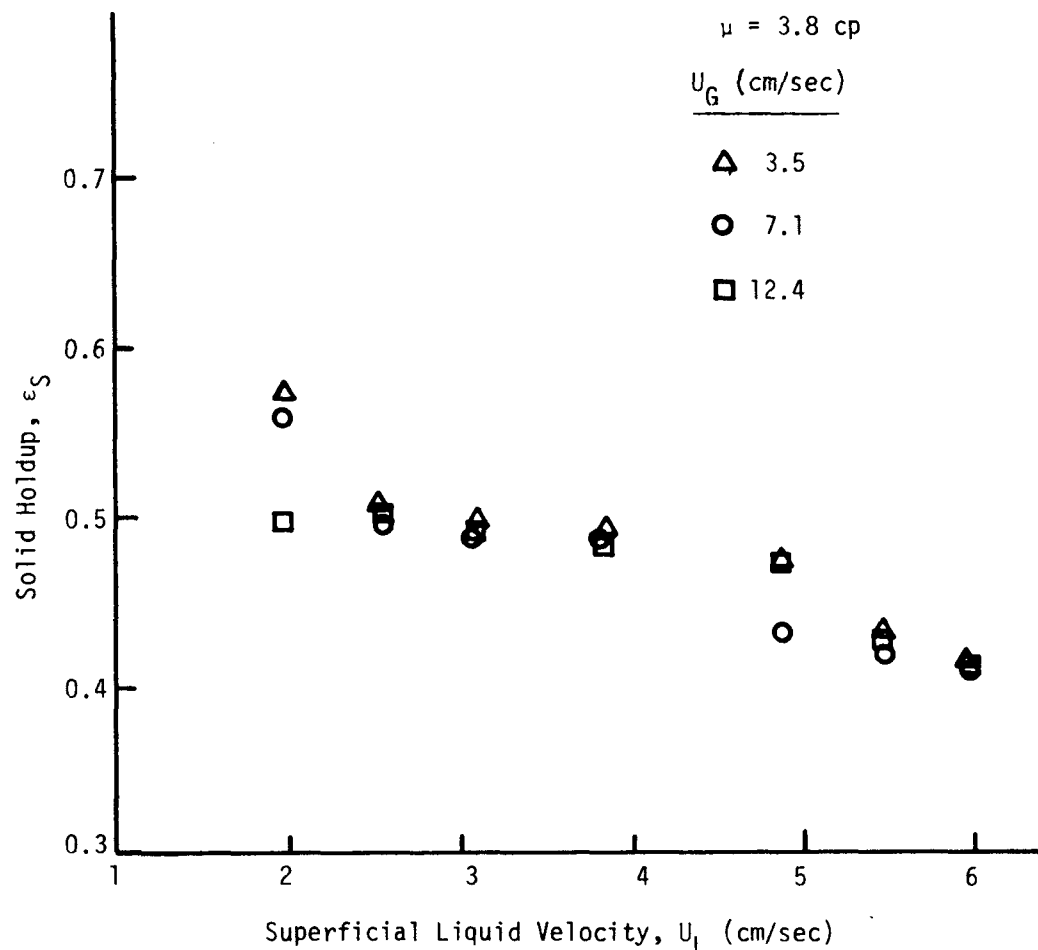




MASSACHUSETTS INSTITUTE OF TECHNOLOGY  
SCHOOL OF CHEMICAL ENGINEERING PRACTICE  
AT  
OAK RIDGE NATIONAL LABORATORY

EFFECT OF SUPERFICIAL LIQUID  
VELOCITY ON PHASE HOLDUPS

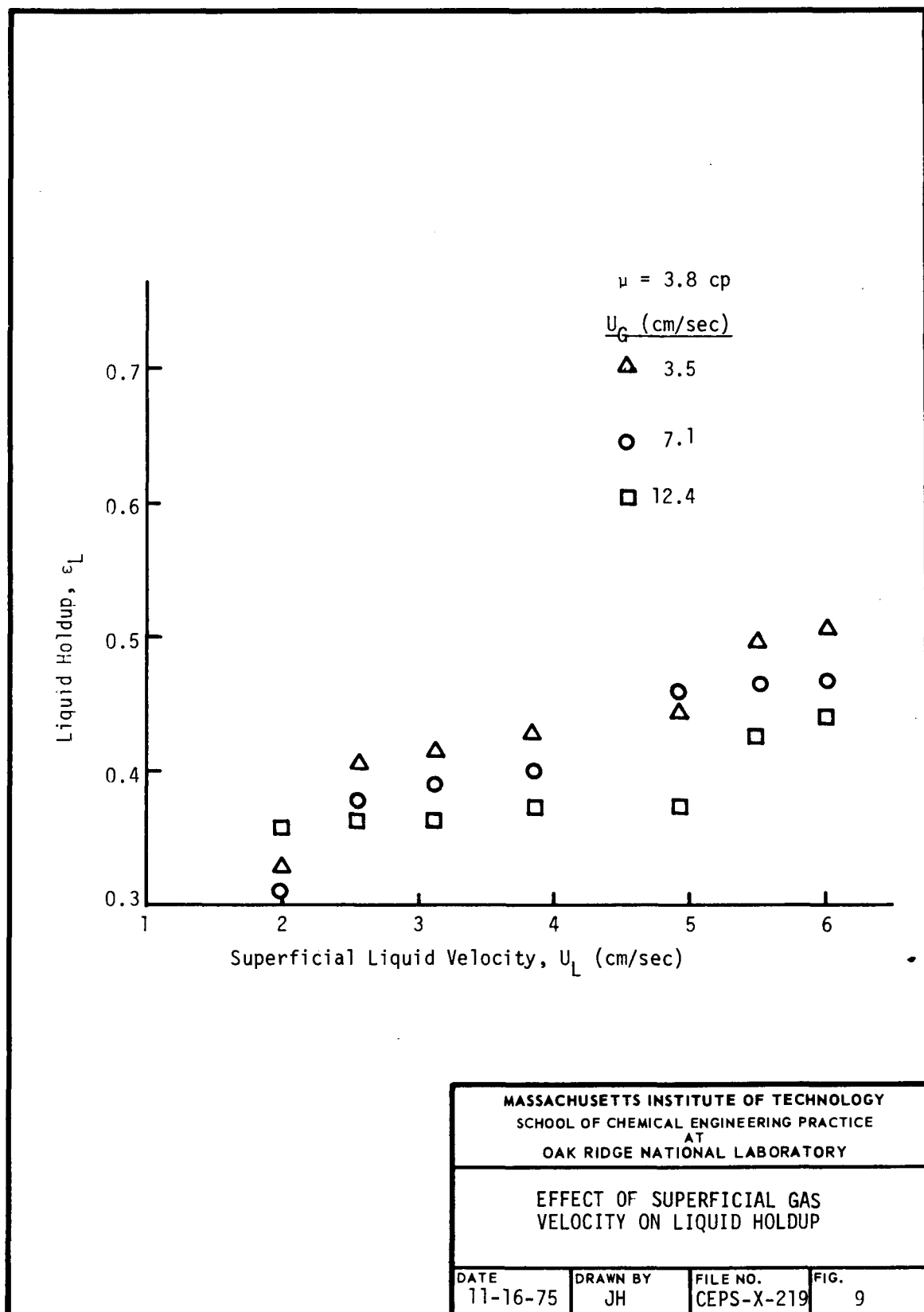
DATE 11-16-75	DRAWN BY JH	FILE NO. CEPS-X-219	FIG. 7
------------------	----------------	------------------------	-----------

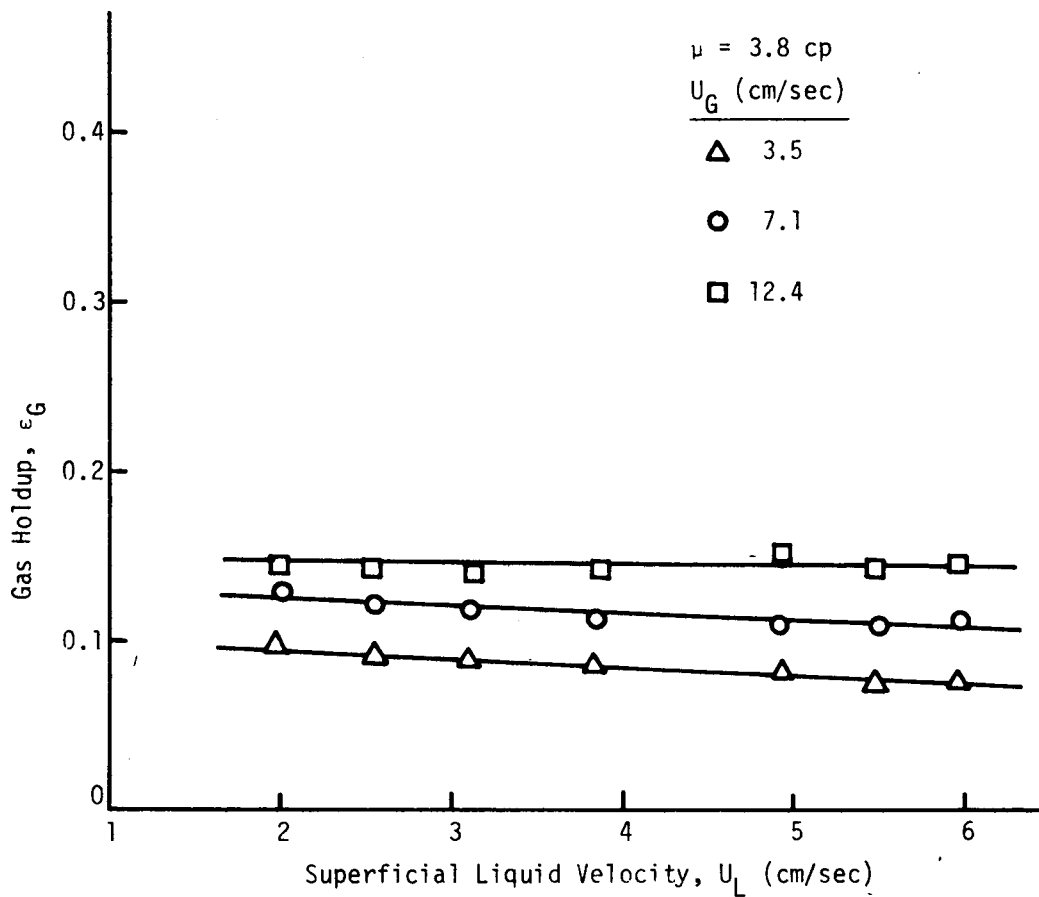


MASSACHUSETTS INSTITUTE OF TECHNOLOGY  
SCHOOL OF CHEMICAL ENGINEERING PRACTICE  
AT  
OAK RIDGE NATIONAL LABORATORY

EFFECT OF SUPERFICIAL GAS  
VELOCITY ON SOLID HOLDUP

DATE 11-16-75	DRAWN BY JH	FILE NO. CEPS-X-219	FIG. 8
------------------	----------------	------------------------	-----------

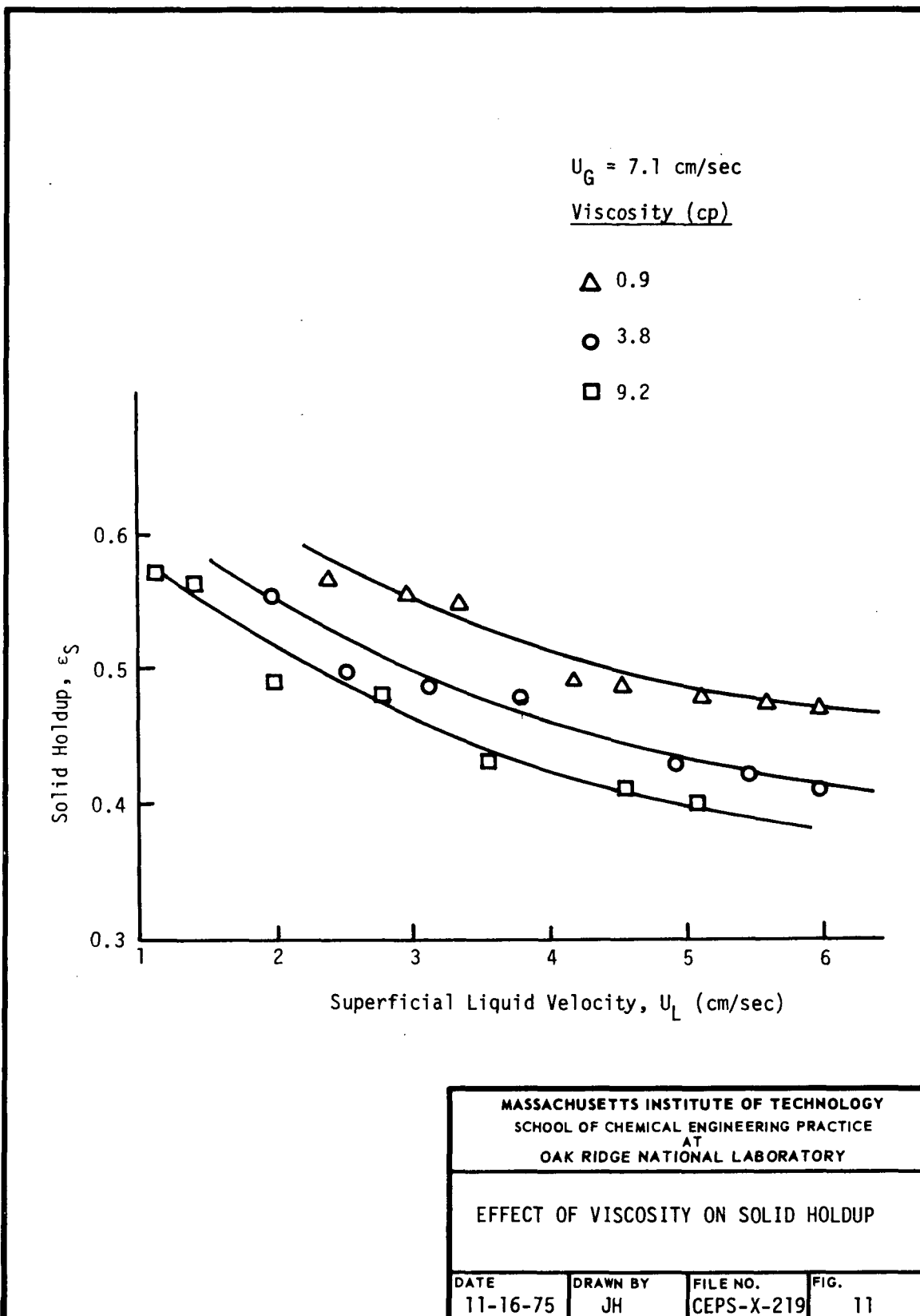


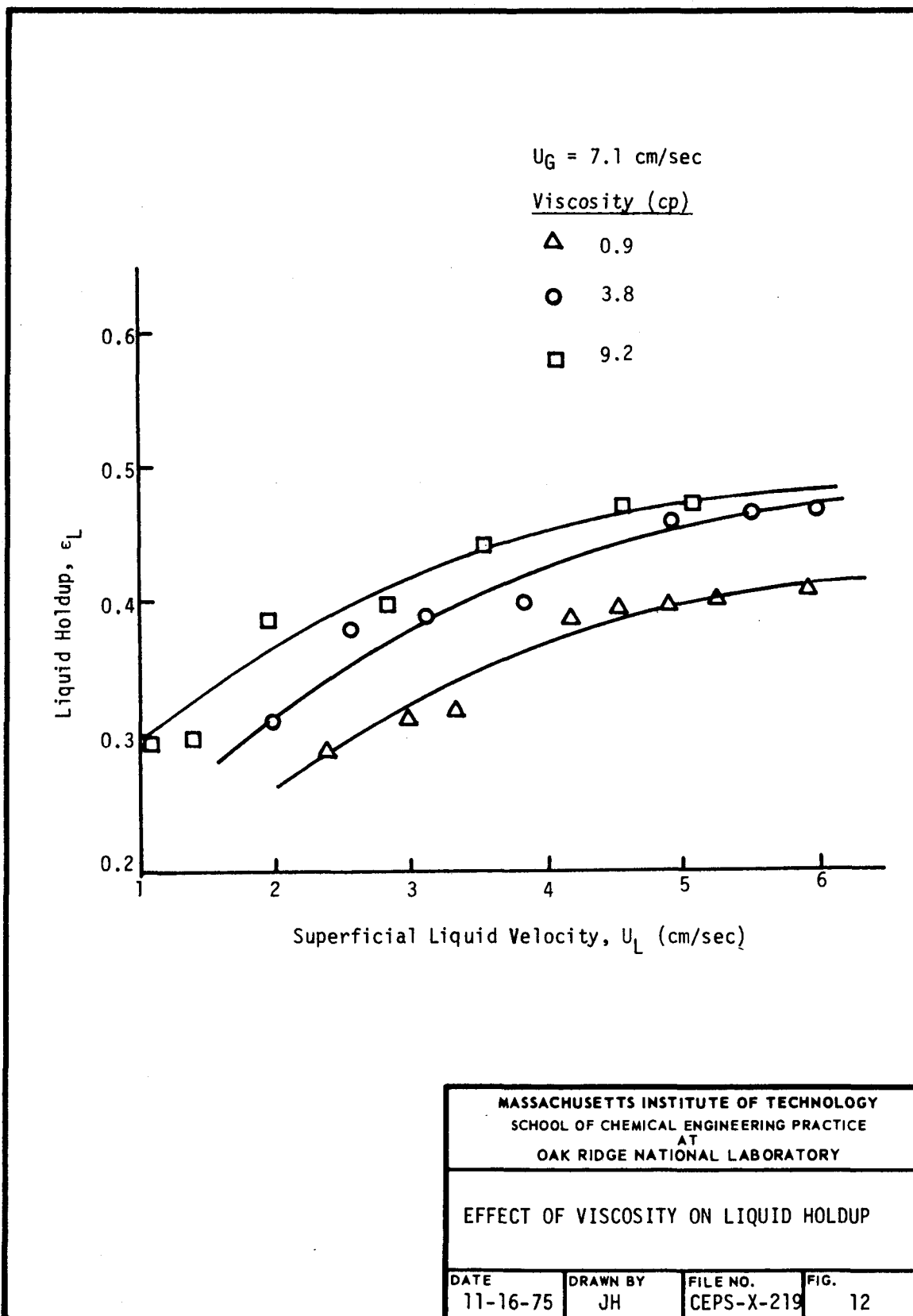


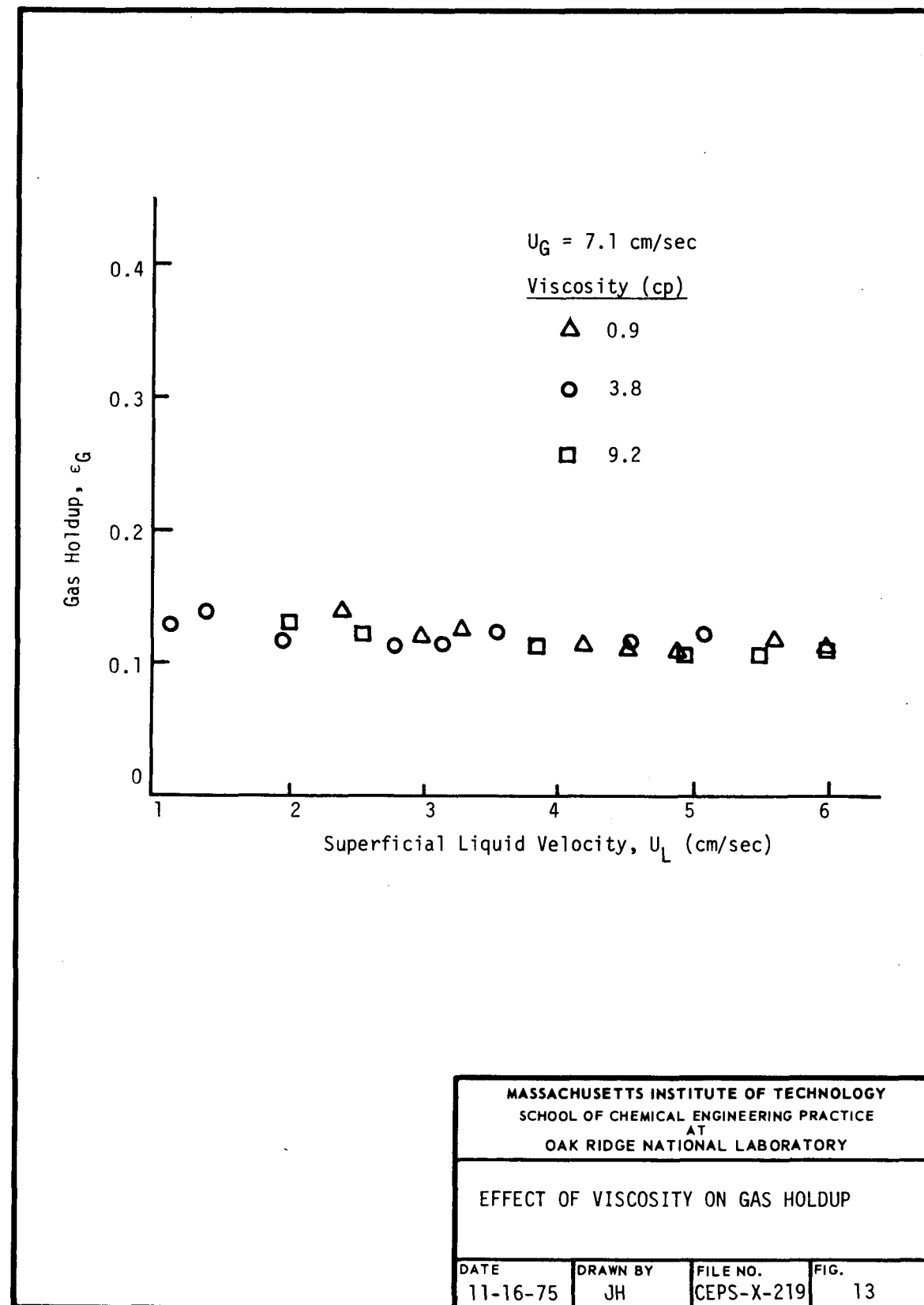
MASSACHUSETTS INSTITUTE OF TECHNOLOGY  
 SCHOOL OF CHEMICAL ENGINEERING PRACTICE  
 AT  
 OAK RIDGE NATIONAL LABORATORY

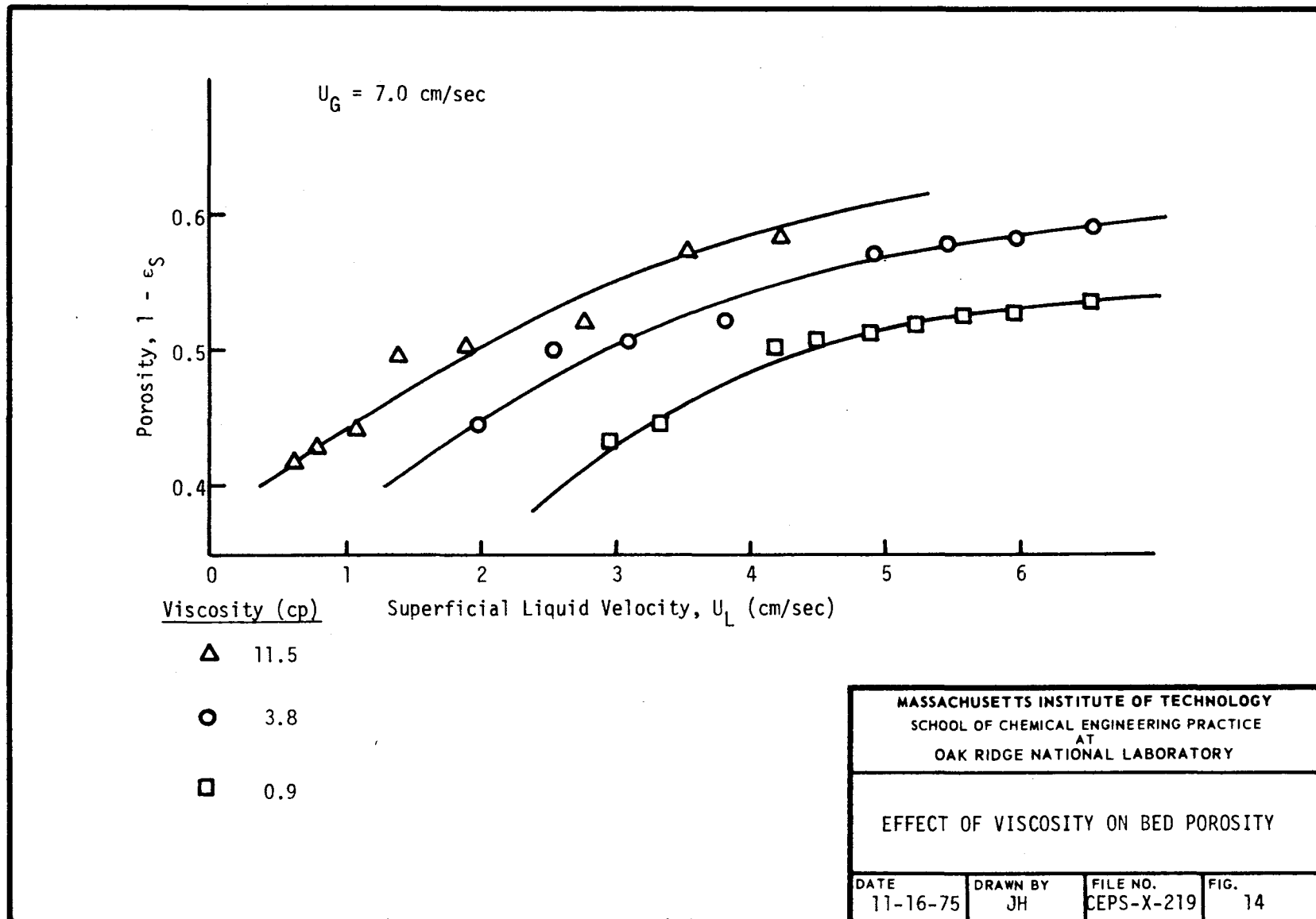
EFFECT OF SUPERFICIAL GAS  
 VELOCITY ON GAS HOLDUP

DATE 11-16-75	DRAWN BY JH	FILE NO. CEPS-X-219	FIG. 10
------------------	----------------	------------------------	------------









at any one set of operating conditions must suffice. Kline and McClintock (10) have derived an expression for evaluating the uncertainty interval associated with such single sample experiments. If  $Q$  is a function of  $n$  independent variables,

$$Q = f(q_1, q_2, \dots, q_n) \quad (11)$$

The uncertainty associated with  $Q$  is given by:

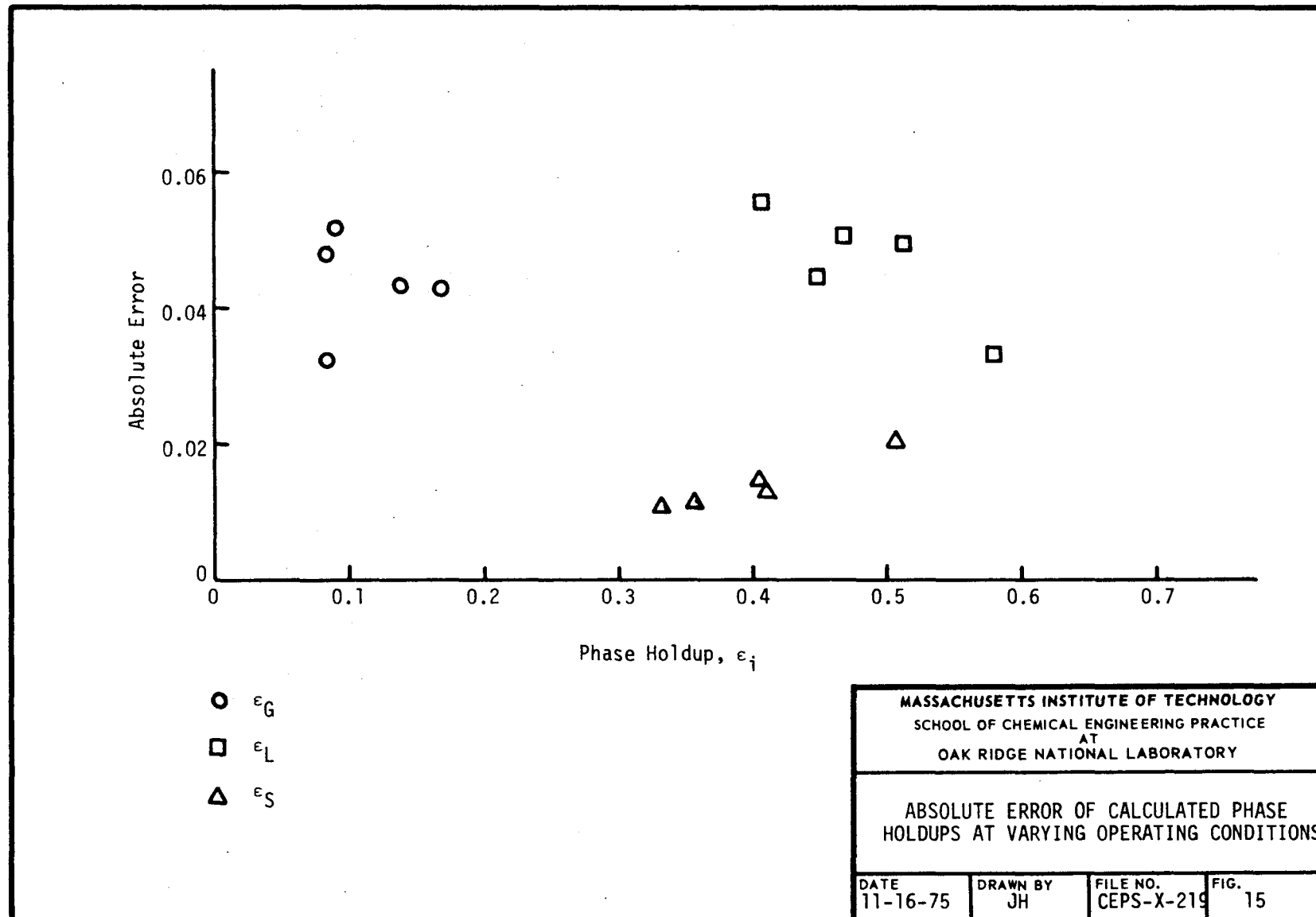
$$\Delta Q = \left[ \sum_{i=1}^n \left( \frac{\partial f}{\partial q_i} \Delta q_i \right)^2 \right]^{1/2} \quad (12)$$

where  $\Delta q_i$  is the uncertainty associated with each of the independent variables.

This method was applied in determining the uncertainty associated with each of the calculated phase holdups. The phase holdups were functions of the independent variables presented in Eqs. (6), (7), and (8). The uncertainties intrinsic to each of these independent terms could be estimated statistically or from the observed limitations of the measuring apparatus. The particular equations from which the uncertainties associated with the phase holdups were calculated are presented in Appendix 8.1.

Error analyses were not performed for all calculated values of the phase holdups. Instead, the holdups selected for analysis were based on a factored design of the experimentation. The holdups analyzed represented those at the maximum and minimum bounds of the experimental operating conditions. The error analysis was also extended to include the data obtained by Khosrowshahi *et al.* (8) with 8x12 and 4x8 mesh alumina-water-air fluidized systems.

The absolute value of the error for each of the phase holdups was found to be essentially constant over a wide range of operating conditions, as shown in Fig. 15. The average absolute error was 0.018 for the solid holdup, 0.056 for the gas holdups, and 0.058 for the liquid holdup. This corresponds to an average relative error of 4% for the solid holdup, 14% for the liquid holdup, and 54% for the gas holdup. The major sources of these experimental errors were identified. For the solid holdup, over 50% of the error was attributed to the error in measuring the solid density and over 40% to the error in calculating the bed height. The errors associated with the mass of solid in the bed and the column area were negligible. Furthermore, the error in the solid density accounted for over 40% of the error associated with the gas holdup, the remainder resulting from the uncertainty associated with the calculation of the bed pressure gradient. The error in the liquid holdup is directly related to the errors in the other two phase holdups (see Appendix 8.1).



### 4.3 Correlation of Hydrodynamic Variables

#### 4.3.1 Approach

The phase holdups and liquid minimum fluidization velocity were correlated with the operating parameters of the fluidized bed. The operating parameters available for correlation were:  $U_G$ ,  $U_L$ ,  $d_p$ ,  $\rho_S$ ,  $\rho_L$ ,  $\rho_G$ ,  $\sigma_L$ ,  $\mu_L$ ,  $D_C$ , and  $U_{Lmf}$ . A step-wise multi-variable correlation procedure was followed using product forms of both dimensional and non-dimensional variables. This step-wise process consisted of determining a correlation for the phase holdups or minimum fluidization velocity utilizing initially all the available parameters. The least significant of these variables based on the correlation *t*-values was eliminated, and the correlation repeated. The number of dimensional variables was reduced by this technique, allowing for a reduction in the number of non-dimensional groups conceivably formed and establishing the functional dependencies of the remaining significant variables. Dimensionless groups which reflected the relationships of these remaining dimensional variables were formed and the process repeated.

In the multi-step method it was necessary to define or select the best correlation. The correlation coefficient indicated the agreement between the calculated and experimental values of the phase holdups and minimum fluidization velocity. However, this coefficient is maximized by increasing the number of adjustable parameters, i.e., the number of variables used in the correlation. It was desirous to represent the hydrodynamic variables only in terms of the significant operating parameters, eliminating those contributing marginally to the correlation. Therefore, the selection criteria for the correlation of the hydrodynamic variables were to choose the correlation having the highest correlation coefficient and consisting of not more than two non-dimensional terms. A third term would be included only if it significantly improved the correlation coefficient, thereby representing an actual operating dependency. Furthermore, if the transition from the dimensional to the dimensionless variables could not be accomplished without a significant reduction in the correlation coefficient, then the correlation was presented in terms of the dimensional variables to indicate the basic relationships of the operating conditions to the hydrodynamic variables.

Correlations were derived for three different sets of data. The first set consisted of 229 specific sets of experimental data obtained in this investigation covering a wide range of liquid velocities and phase properties. The second set included the 105 sets of operating conditions reported by Khosrowshahi *et al.* (8). This combined set, a total of 334 points, represents the data taken at ORNL using the same experimental apparatus and techniques. The third set of data corresponds to the 1223 points extracted from literature sources (1, 2, 4, 6, 9, 11, 12, 13). The data reported in the literature sources do not, however, include all three phase holdups at each set of operating conditions, nor the minimum fluidization velocities. The data, a total of 1557 sets of operating conditions, do cover a wide range of operating conditions and phase properties in three-phase fluidized beds.

A multiple linear regression program, CORRLT, was written to perform product-form correlations of both the dimensional and non-dimensional variables important in a three-phase fluidized bed. This program is described in detail in Appendix 8.3.

#### 4.3.2 Solid Holdup

The porosity of the fluidized bed was correlated by the multi-step procedure. This process demonstrated that the major dimensional variables affecting the solids holdup were the liquid velocity and viscosity, and the solid density and particle diameter. The functional relationship between these variables could be approximated by the following equation:

$$1 - \epsilon_S \propto \frac{U_L \mu_L^{0.5}}{d_p \rho_S^{0.5}} \quad (13)$$

On the basis of this functionality, several non-dimensional groups were formed. Correlations for the bed porosity were performed with each of the three data bases: the experimental data, all ORNL data, and all available data. From the experimental data only, the best correlation, based on the selection criteria previously established, was:

$$1 - \epsilon_S = 1.03 F_L^{0.094+0.003} G_a^{-0.026+0.001} \quad (1)$$

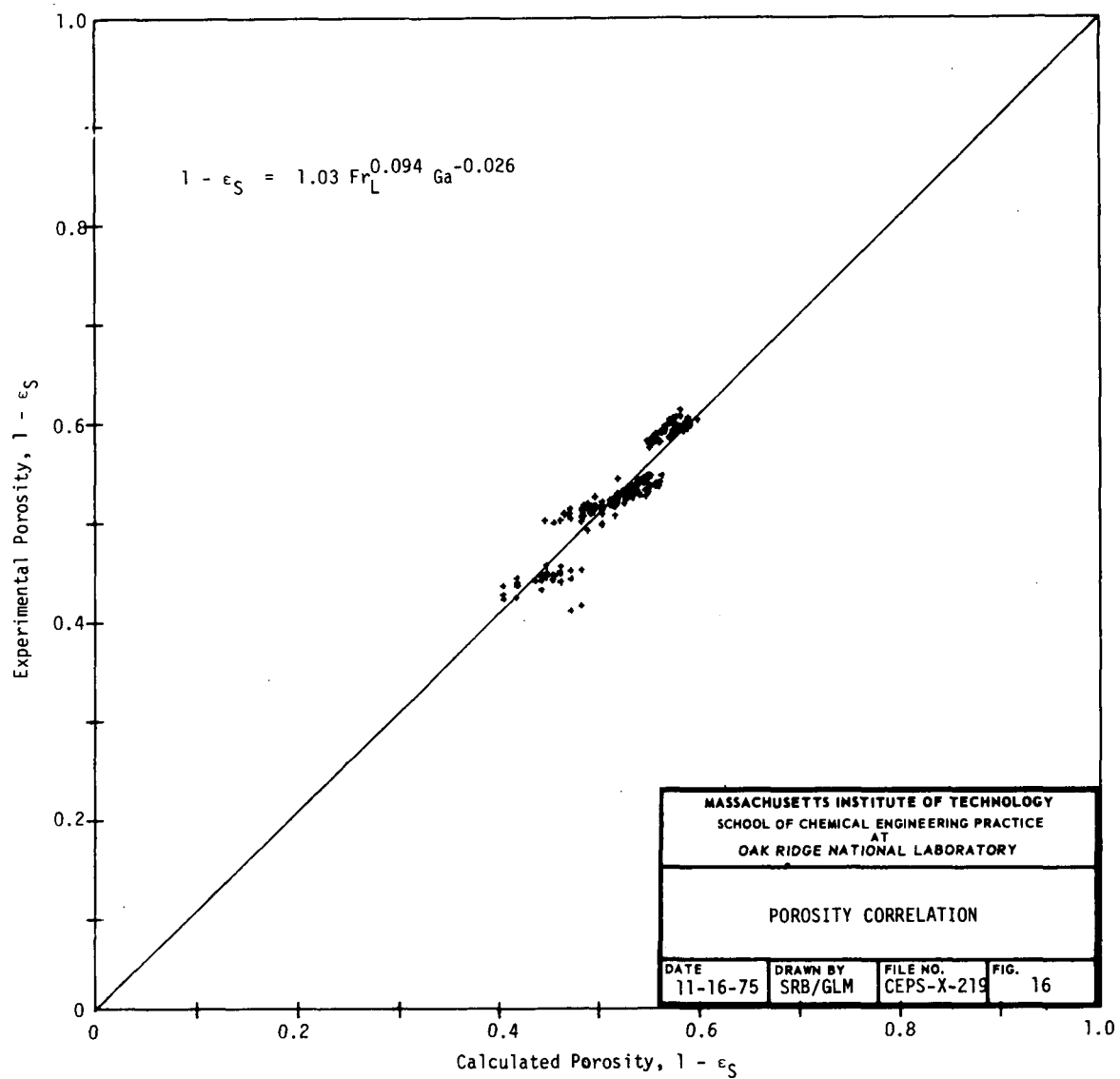
The correlation coefficient for this equation was 0.931, and the F-value was 7.37. The agreement between the calculated and experimental porosities is shown in Fig. 16.

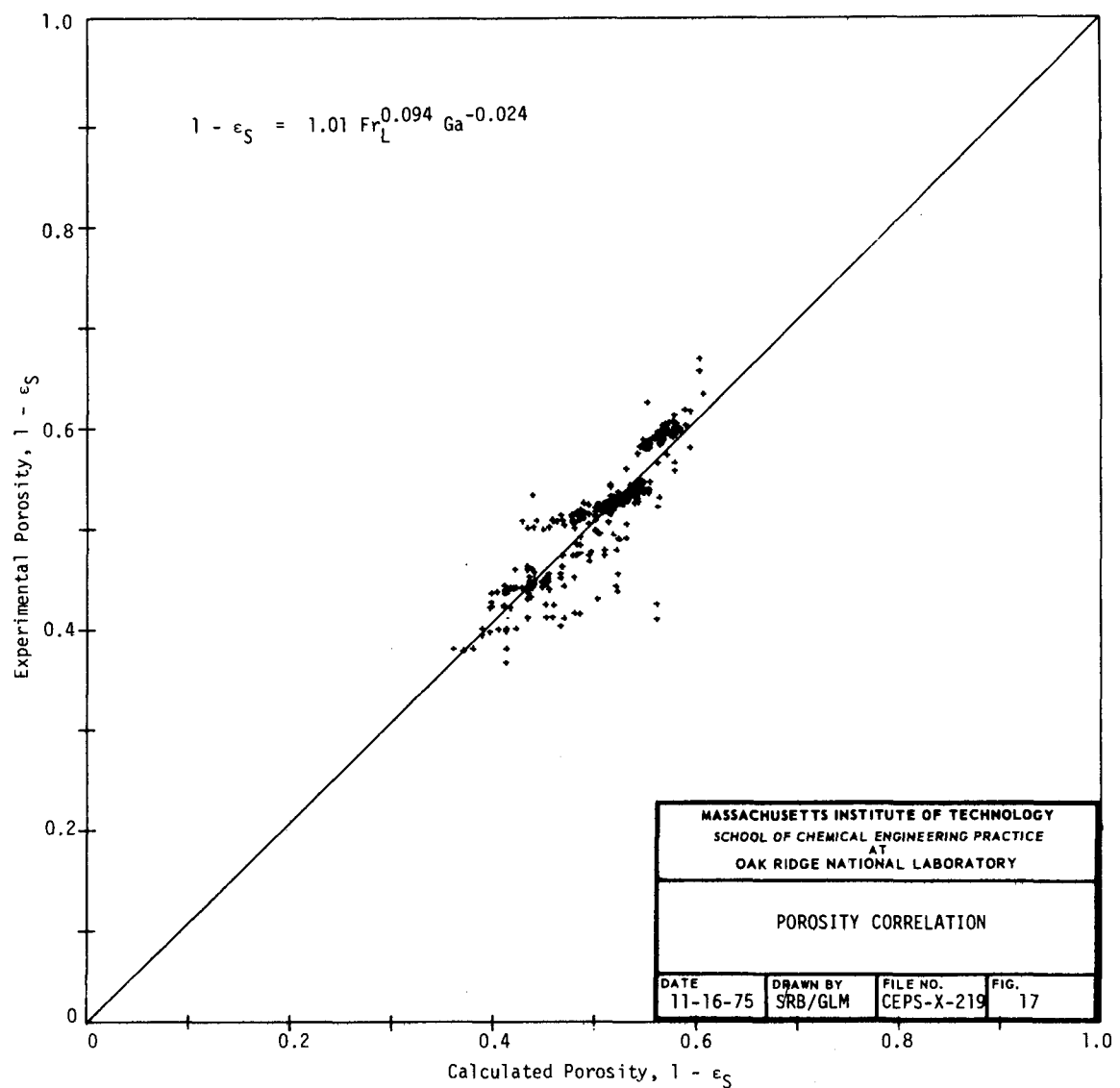
On combining the experimental data with that of Khosrowshahi et al. (8), a similar correlation for the bed porosity was determined:

$$1 - \epsilon_S = 1.01 F_L^{0.094+0.003} G_a^{-0.024+0.002} \quad (14)$$

The correlation coefficient, 0.886, is somewhat less than that obtained without including Khosrowshahi's data. The resulting scatter in the data, as shown in Fig. 17, may demonstrate restrictions on the general applicability of the correlation. However, Khosrowshahi et al. (8) may have experienced some difficulty in accurately quantifying the solids attrition which occurred during his experimentation and this may account for some of the scatter in his porosity data. Considering the experimental difficulties, the agreement between the two sets of data is quite good.

The data from above were included with data extracted from the literature (1, 2, 4, 6, 9, 11, 12, 13) to cover a wider range of operating





conditions, and correlated as before. However, the best correlation for these data is of a different form than that previously determined:

$$1 - \epsilon_S = 1.53 \text{ Re}_L^{0.275+0.005} \text{ Ga}^{-0.171+0.003} \quad (2)$$

This correlation is somewhat worse than the previous ones as indicated by the correlation coefficient of 0.842 and inspection of Fig. 18. The scatter in these data may be attributed to the wide range and different regimes of operation, the different measurement techniques used by various authors in their experimentation, and to an improper correlation form. Furthermore, it appears that the derived correlation does not adequately describe the effect of the gas velocity on the porosity. This is illustrated by the vertical strings of data apparent in Fig. 18 representing sets of operating conditions varying only in gas velocity.

The differences between the correlating groups in the experimental data may be explained by examining the dimensional form of Eqs. (1) and (2). Equation (2) which incorporated the literature data is more dependent on the liquid velocity and particle diameter. This was expected considering the limited velocity ranges obtainable in the experimental apparatus, and the absence of any variation in the solid properties in this investigation.

#### 4.3.3 Gas Holdup

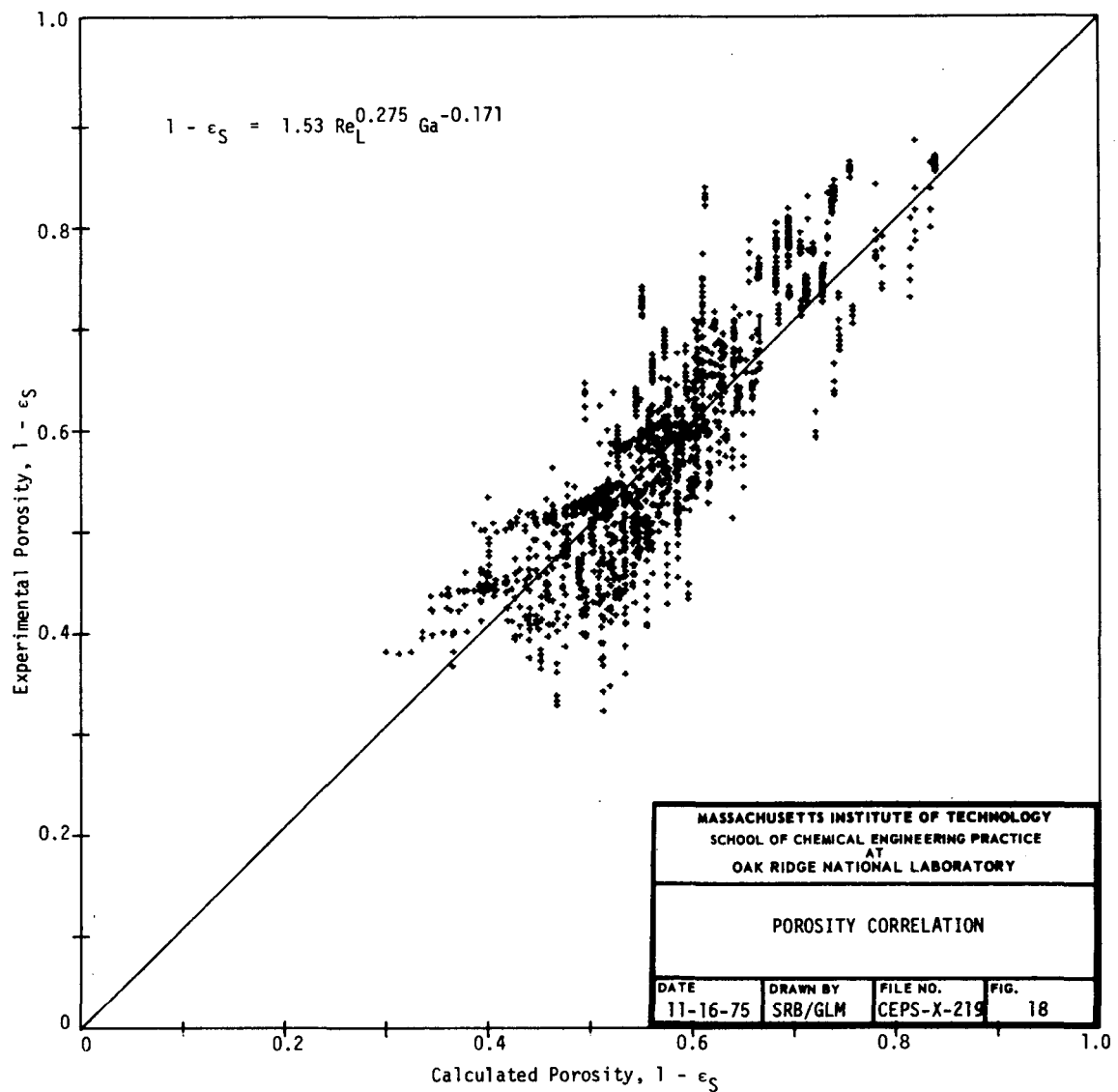
The gas holdup was correlated using only the experimental data. A correlation was derived which reflects the relative independence of the gas holdup with liquid velocity and viscosity and the dominant effect of the gas velocity:

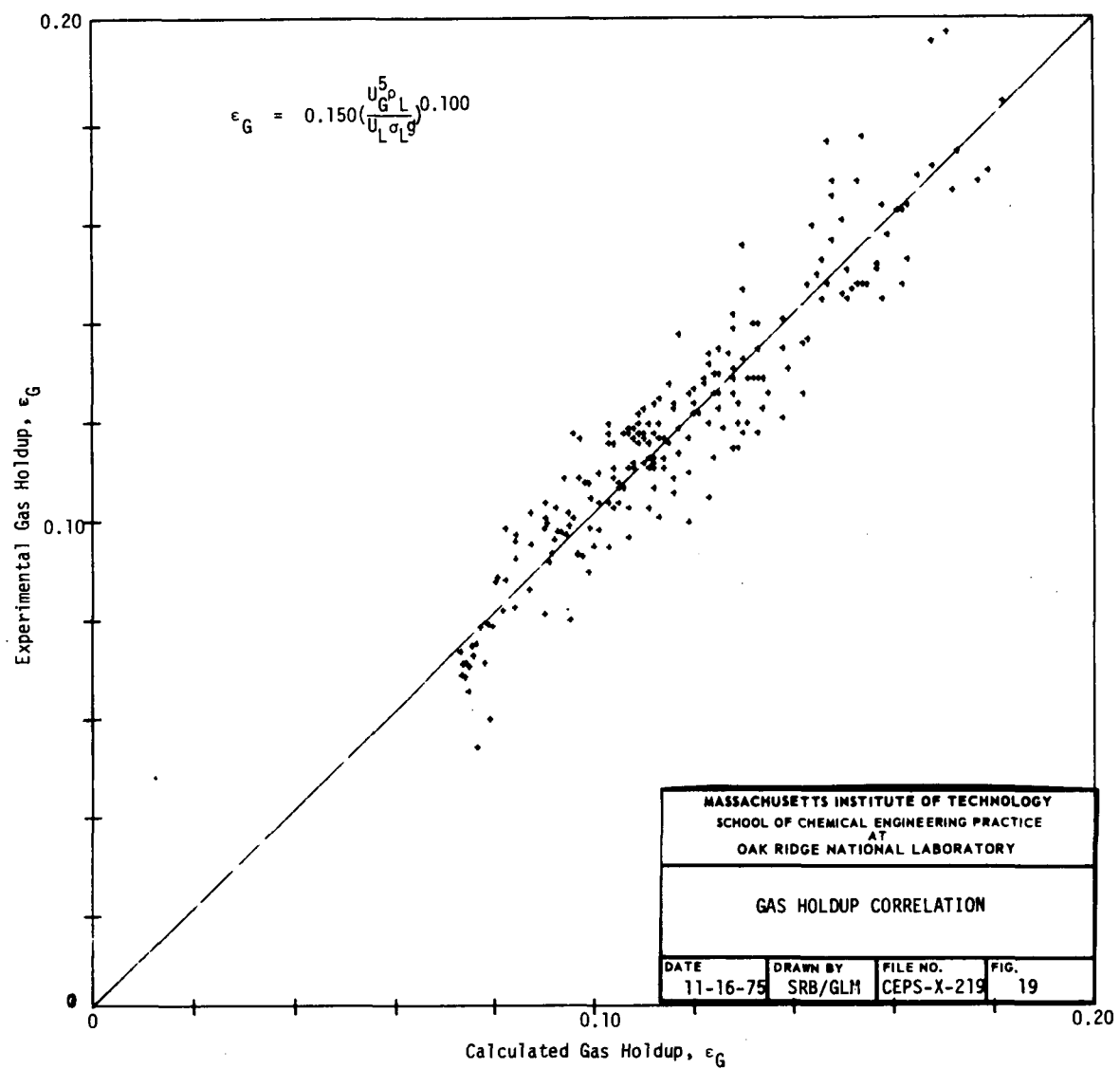
$$\epsilon_G = 0.150 \left( \frac{U_G}{U_L} \right)^5 \frac{\rho_L}{\sigma_L g} 0.100+0.003 \quad (3)$$

The correlation coefficient for Eq. (3) is 0.934. This correlation is similar in form to one proposed by Ferguson (7) describing the gas holdup. There is an excellent fit between the experimental data and the holdups predicted by this correlation as shown in Fig. 19. No correlation could be obtained for the gas holdup when the data base was expanded to include that of Khosrowshahi *et al.* (8). Furthermore, no reliable information on the gas holdup was present in the literature data compiled.

#### 4.3.4 Liquid Holdup

Correlations for the liquid phase holdup were developed in a manner similar to those for the solid phase. The correlations were developed only for the experimental data and for the ORNL data. Little data for the liquid holdup were available in the literature, due possibly to the relative complexity of the experimental techniques involved.





For the liquid holdup the following dimensional correlation was obtained from the experimental data:

$$\epsilon_L = 0.45 U_L^{0.269+0.007} U_G^{-0.146+0.010} (\rho_S - \rho_L)^{-1.072+0.034} \quad (4)$$

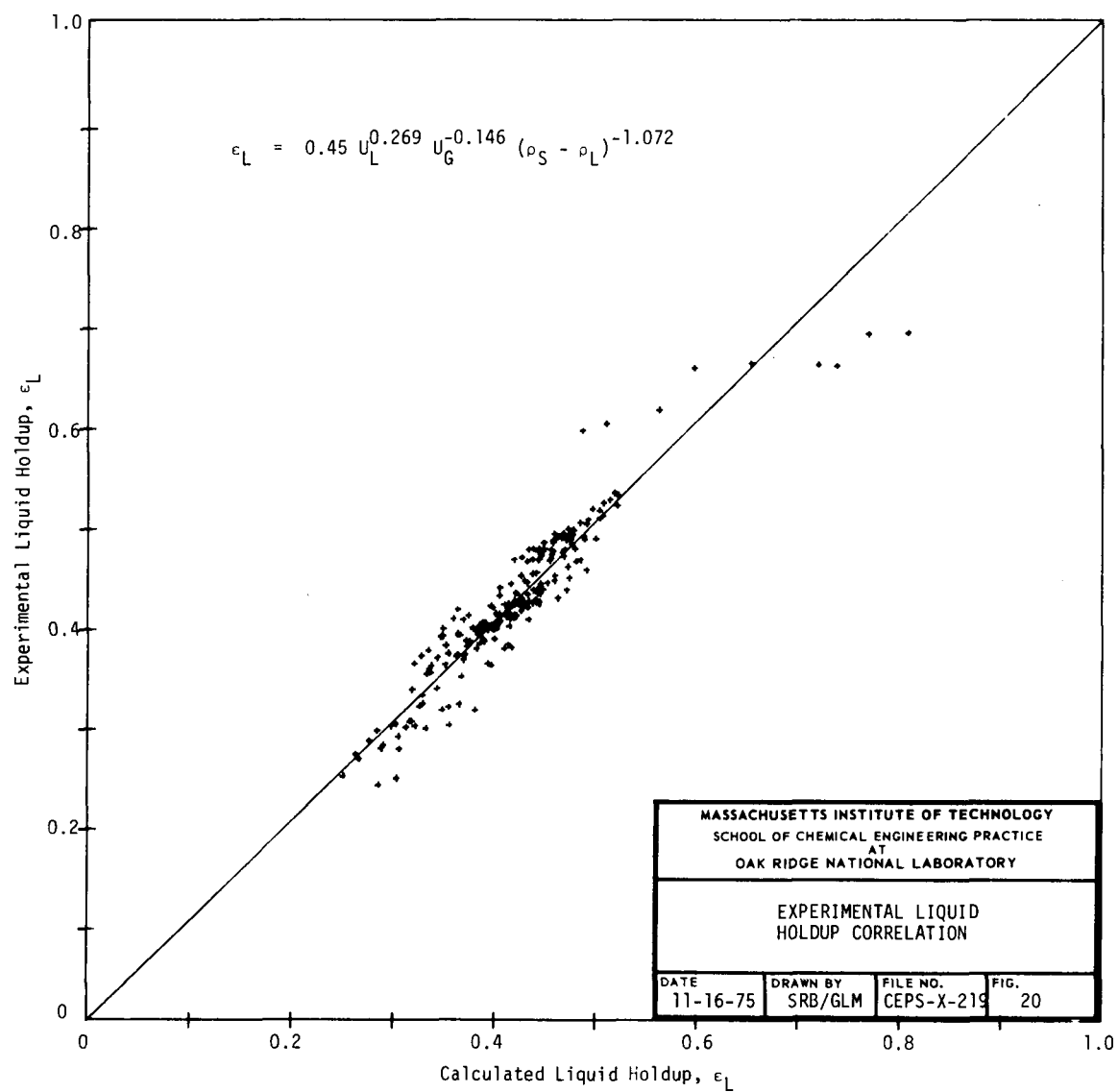
This equation has a correlation coefficient of 0.944, and as can be seen in Fig. 20, there exists excellent agreement between the experimental and calculated values for the liquid holdup.

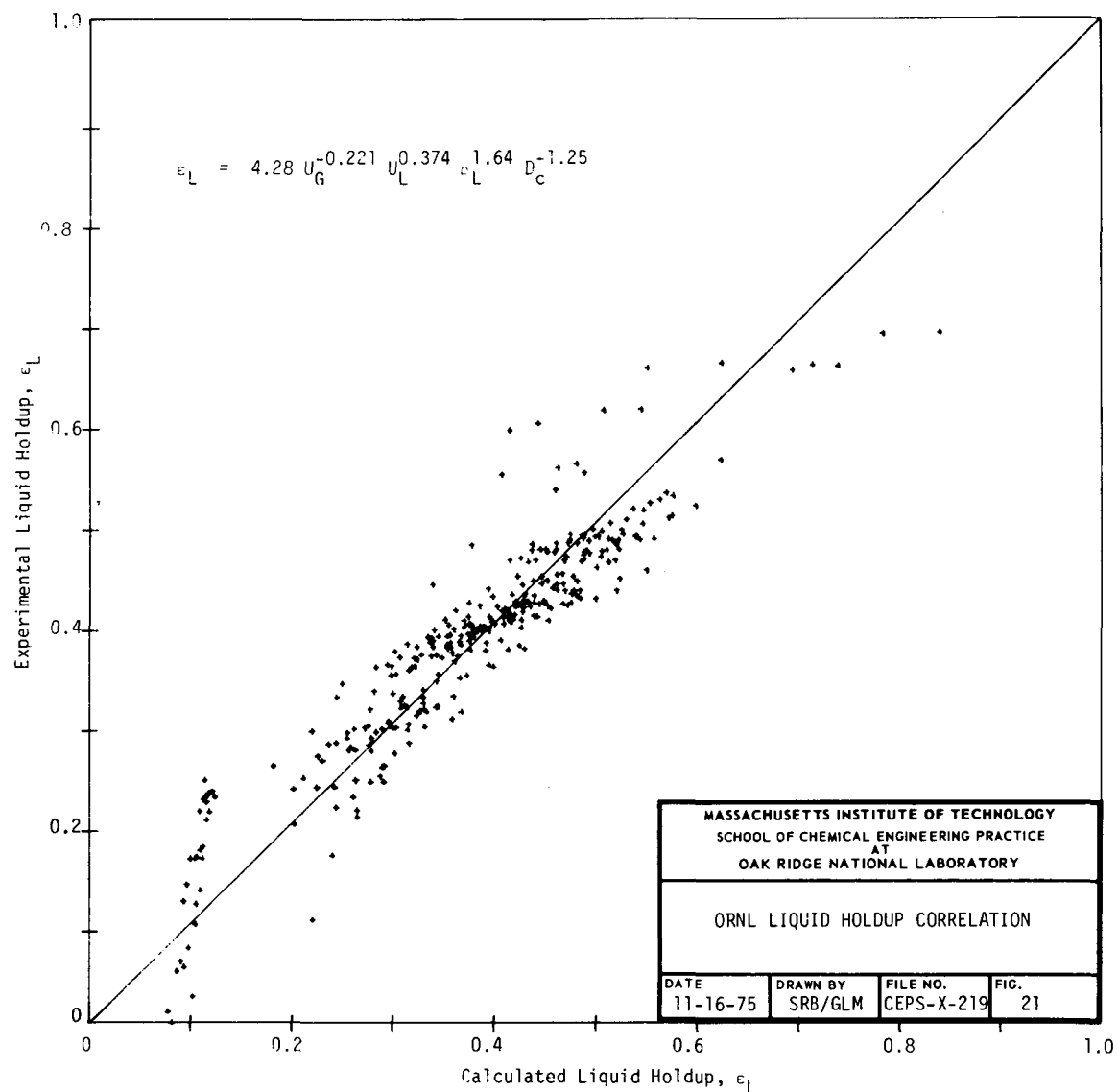
Using all the ORNL data, the following dimensional correlation for the liquid holdup was derived:

$$\epsilon_L = 4.28 U_L^{0.374+0.036} U_G^{-0.221+0.032} \rho_L^{1.64+0.22} D_c^{-1.25+0.11} \quad (15)$$

Even with the additional number of parameters, this correlation is significantly worse than that obtained with only the experimental data. This can be seen by comparison of Figs. 20 and 21 and the correlation coefficients of 0.944 and 0.782. The inability to correlate the ORNL data together may signify that the liquid holdup may not be represented by a product form correlation. However, it may be due in part to errors inherent in the liquid holdup calculation technique used by Khosrowshahi *et al.* (8). The liquid holdup was calculated in Eq. (7) using the bed pressure drop as determined by the intersection of the two lines in Fig. 2. However, as can be seen in this figure, there is some curvature in the points near the apex, which is a result of a non-uniform solid holdup throughout the bed. In this investigation, this effect was considered to be an end effect only, caused by solid entrainment near the top of the bed, and therefore not applicable in the determination of a general liquid holdup value. The geometric effects of the bed height were not considered in the calculation of the liquid holdup. Khosrowshahi *et al.* (8), however, included this end effect in the determination of the bed pressure drop, with the result that the liquid holdups reported were greater than was representative of the actual physical situation. The correlation for the liquid holdup derived from the ORNL data was a function of the column diameter. This diameter dependence may illustrate a bubble flow effect. However, the sign on the exponent of the diameter term indicates that it is a result of this end effect calculation. Solids entrainment is less pronounced at the lower superficial fluid velocities obtained in Khosrowshahi's larger diameter column. This results in less curvature in Fig. 2, a higher measured pressure drop, and a smaller liquid holdup; thus, calculated liquid holdup varies inversely with column diameter in Eq. (15).

Several non-dimensional correlations for the liquid holdup were attempted. However, due to the form of the dimensional correlations, notably in the density exponent, no dimensionless correlation could be obtained without significant reduction in the correlation coefficient. Furthermore, no correlation reflecting the viscosity effect on the liquid holdup, as shown in Sect. 4.1.3, could be determined.





#### 4.3.5 Minimum Fluidization Velocity

In a three-phase fluidized bed, the minimum fluidization velocity is a combination of both a gas and liquid velocity. In both this investigation and that of Khosrowshahi *et al.* (8), a minimum liquid fluidization velocity was calculated based on data where the liquid velocity was varied while the gas velocity was held constant. This liquid velocity was calculated in a manner described in Appendix 8.2.3 and shown on Fig. 3. Because of the limited amount of data available, correlations could be attempted only for the complete ORNL data. The dimensional correlation obtained for the liquid minimum fluidization velocity:

$$U_{Lmf} = 0.040 \rho_S^{3.75+0.14} U_G^{-0.140+0.020} \mu^{-0.497+0.013} D_c^{-0.423+0.067} \quad (16)$$

had a correlation coefficient of 0.917. Further application of the multi-step process results in the following correlation:

$$U_{Lmf} = 0.014 \rho_S^{3.70+0.153} \mu^{-0.473+0.015} \quad (5)$$

The correlation coefficient for Eq. (5) is 0.877. No dimensionless groups attempted had a comparable fit to the data. It should be noted that in the operating range studied, the minimum fluidization point is independent of the gas velocity. However, the restricted range of the experimentation, in terms of both operating parameters and phase properties, should be considered prior to application of the minimum fluidization correlation to any other fluidized system or operating regime.

## 5. CONCLUSIONS

1. The solid holdup,  $\epsilon_S$ , is a function of the liquid velocity and viscosity. However, over the operating ranges examined, the solid holdup is independent of the gas flow rate. Correlations for the solid holdup were obtained. The best correlation for the ORNL data was:

$$1 - \epsilon_S = 1.03 F_L^{0.094+0.003} G_a^{-0.026+0.001} \quad (1)$$

The best correlation for all data collected and compiled was:

$$1 - \epsilon_S = 1.53 R_L^{0.275+0.005} G_a^{-0.171+0.003} \quad (2)$$

The difference in the two solid holdup correlations is a result of different operating regimes and a lack of variation of the solid phase in the ORNL data.

2. The liquid holdup,  $\epsilon_L$ , is a function of both the gas and liquid velocities. The best correlation for the liquid holdup was:

$$\epsilon_L = 0.45 U_L^{0.260+0.007} U_G^{-0.146+0.010} (\rho_S - \rho_L)^{-1.072+0.034} \quad (4)$$

This holdup is a strong function of the calculation technique or the assumptions involved in calculating the pressure drop across the bed.

3. The gas holdup,  $\epsilon_G$ , is a predominantly a function of the superficial gas velocity:

$$\epsilon_G = 0.15 \left( \frac{U_G^5 \rho_L}{U_L \sigma_L g} \right)^{0.100+0.003} \quad (3)$$

4. The minimum liquid fluidization velocity is a function of the viscosity. For the range of experimental gas velocities studied, the minimum fluidization point is independent of gas velocity. The best correlation for the minimum liquid fluidization velocity was:

$$U_{Lmf} = 0.014 \rho_S^{3.701+0.153} \mu^{-0.473+0.015} \quad (5)$$

## 6. RECOMMENDATIONS

1. A more comprehensive study would involve the variation of alternative operating parameters indicated as potentially significant by this study. In the experimentation conducted at ORNL, there has been little variation of the solid density or particle size. This omission may be a cause of the difference between the two solid holdup correlations obtained [Eqs. (1) and (2)]. Furthermore, liquid density and surface tension have been held effectively constant for all studies of three-phase fluidized beds, even though the importance of these factors was demonstrated in the correlations for the liquid and gas phase holdups. Variation of these parameters is necessary for verification of the current correlations and for identification of other operating dependencies.

2. Further studies at lower superficial gas velocities should be conducted to verify the extrapolation of the minimum fluidization line to two-phase flow.

3. Further correlations, particularly of a non-product form, should be attempted. These other correlation forms may allow consideration of the limiting holdup values at the extremes of the operating conditions. Furthermore, non-product correlation forms may be required to accurately describe the liquid holdup and the gas velocity effect on the solid holdup.

4. A thorough investigation of the effect of bed geometry on the hydrodynamic variables is required to substantiate scaleup procedures and even to permit comparisons between bench-scale operation. There was some evidence in the correlation for minimum fluidization velocity which indicated that the column diameter may be an important operating parameter. Furthermore, the bed height may be important, particularly for short bed heights. For these heights, entrainment end effects at the top of the bed may be significant when using low density solids or high fluid flow rates. There is also an entrance effect due to poor distribution of the fluids at the base of the column, an effect which may not be negligible for short beds.

Preliminary work with different bed heights at otherwise constant operating conditions indicates that this variable may be a factor causing the measured pressure gradient within the bed.

5. More care should be taken in determining the solid density in future work, as this term was shown to be the major source of error in the experimental results.

6. Alternative holdup measurement techniques may be employed to validate or facilitate the current experimental procedures. Possible techniques include conductivity or tracer studies for determining the liquid holdup and volumetric techniques for the gas holdup.

## 7. ACKNOWLEDGMENT

The authors would like to express their appreciation to J.M. Begovich and J.S. Watson for their assistance throughout the project.

## 8. APPENDIX

## 8.1 Error Analysis Calculations

An error analysis was performed for the phase holdups which were calculated by the following set of equations:

$$\epsilon_S = \frac{M_S}{\rho_S \Delta H_B} \quad (6)$$

$$\epsilon_G = \frac{\left(\frac{H_B + \Delta h_B}{H_B}\right)\rho_L - \epsilon_S \rho_S - \rho_L + \epsilon_S \rho_L}{\rho_G - \rho_L} \quad (17)$$

$$\epsilon_L = 1 - \epsilon_S - \epsilon_G \quad (18)$$

A derivation of these equations is given by Khosrowshahi et al. (8).

For the error analysis calculations, since  $\rho_G \ll \rho_L$ , the gas holdup can be rewritten as:

$$\epsilon_G \approx \epsilon_S \left( \frac{\rho_S}{\rho_L} - 1 \right) - \frac{\Delta h_B}{H_B} \quad (19)$$

The term  $\Delta h_B/H_B$ , representing the calculated pressure gradient through the fluidized bed, is denoted by the term S.

The error associated with each of the holdups was calculated by the general error expression [Eq. (12)] as suggested by Kline and McClintock (10). If Eq. (12) is applied to the different holdup expressions, the errors in the holdup may be expressed in terms of the uncertainties in the experimentally measured quantities:

$$\Delta \epsilon_S = \epsilon_S \left[ \left( \frac{\Delta M_S}{M_S} \right)^2 + \left( \frac{\Delta \rho_S}{\rho_S} \right)^2 + \left( \frac{\Delta A}{A} \right)^2 + \left( \frac{\Delta H_B}{H_B} \right)^2 \right]^{1/2} \quad (20)$$

$$\Delta \varepsilon_G = \left[ \left( \frac{\rho_S}{\rho_L} - 1 \right)^2 (\Delta \varepsilon_S)^2 + \left( \frac{\varepsilon_S}{\rho_L} \right)^2 (\Delta \rho_S)^2 + \left( \frac{\varepsilon_S \rho_S}{\rho_L^2} \right)^2 (\Delta \rho_L)^2 + (\Delta S)^2 \right]^{1/2} \quad (21)$$

$$\Delta \varepsilon_L = [(\Delta \varepsilon_S)^2 + (\Delta \varepsilon_G)^2]^{1/2} \quad (22)$$

The uncertainties in the measurable parameters were determined by the observed limitations on the experimental apparatus and by the deviation of repeated measurements. The values of these errors are:

$$\Delta M_S = 0.1 \text{ gm}$$

$$\Delta A = 0.36 \text{ cm}^2$$

$$\Delta \rho_S = 0.07 \text{ gm/cm}^3$$

$$\Delta \rho_L = 0.002 \text{ gm/cm}^3$$

The uncertainties on the bed height and pressure gradient,  $\Delta H_B$  and  $\Delta S$ , were evaluated for each chosen experimental case by a linear least squares regression for a 95% confidence limit T-value. For experimental Run 25, the values for these terms were:

$$\Delta S = 0.036 \text{ cm fluid/cm bed height}$$

$$\Delta H_B = 1.29 \text{ cm}$$

For Run 25 the operating conditions fixed or calculated were:

$$M_S = 2500 \text{ gm}$$

$$A = 45.6 \text{ cm}^2$$

$$\rho_S = 2.26 \text{ gm/cm}^3$$

$$\rho_L = 1.136 \text{ gm/cm}^3$$

$$H_B = 47.7 \text{ cm}$$

$$\varepsilon_S = 0.508$$

$$\varepsilon_G = 0.086$$

$$\varepsilon_L = 0.406$$

By substituting these corresponding values into Eqs. (20), (21), and (22), the errors in the holdups for this particular case were calculated:

$$\Delta \epsilon_S = 0.021$$

$$\Delta \epsilon_G = 0.052$$

$$\Delta \epsilon_L = 0.056$$

Similar calculations were performed for the other cases selected for analysis.

## 8.2 Computerized Data Analysis

### 8.2.1 Explanation of FLBD

Computer program FLBD accepts experimental data and calculates the fluidized bed height, pressure drop, phase holdups, and minimum liquid fluidization velocity for a set of operating conditions and stores these quantities in three data files. These data files form a portion of the data base for the program CORRLT which forms correlations among these variables. FLBD is an improvement over the previous data analysis programs developed by Khosrowshahi *et al.* (8). FLBD has automated the determination of the bed height and pressure drops by fitting least squares straight lines to experimental manometer readings. The program plots the experimental data and fitted lines for visual inspection. Provisions for eliminating those experimental runs for which insufficient data points are available to construct these lines are outlined in Sect. 8.2.3. Figure 22 illustrates the order of significant operations in FLBD.

### 8.2.2 FLBD Input and Output

The program FLBD requires input data from one experimental run at a constant gas velocity and up to 20 liquid velocities. These data must be stored in file FOR10.DAT prior to the execution of FLBD. The program EXPINP is available to facilitate acceptance and storage of the data in file FOR10.DAT. The experimental data are input into EXPINP according to the following format:

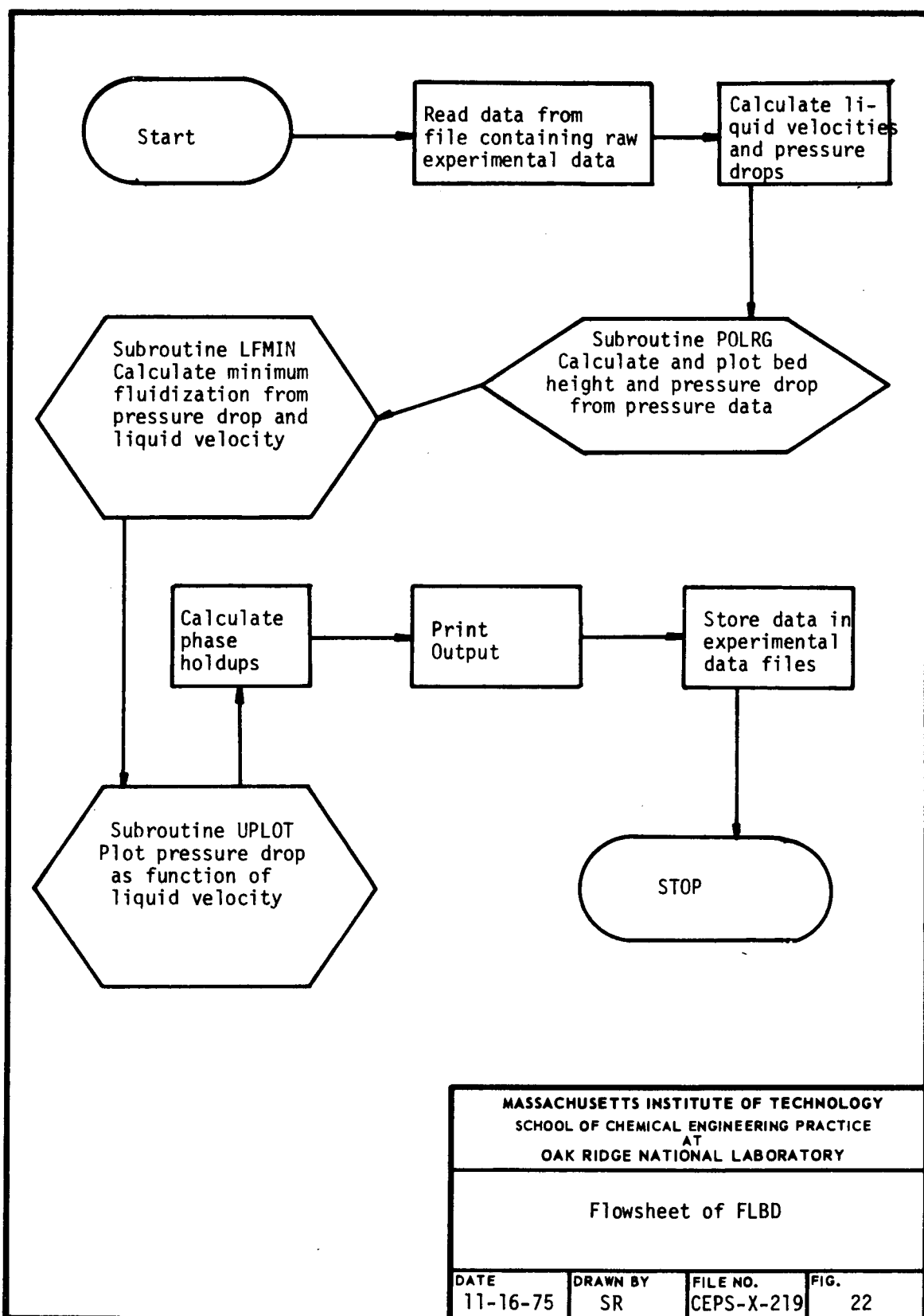
First Line:

RUNQTY the number of lines of manometer readings on the data sheet

DATSHT an identifying data sheet number

DC diameter of the column, in.

PACWT weight of the solid packing in the column, gm



PATM	atmospheric pressure, mm Hg
TLIQ	temperature of the liquid, °C
VISCOS	viscosity of the liquid, cp
RHOG	density of the gas, gm/cm <sup>3</sup>
RHOL	density of the liquid, gm/cm <sup>3</sup>
RHOS	density of the solid, gm/cm <sup>3</sup>
SIGMA	liquid surface tension, dynes/cm
DP	diameter of the solid particle, cm
GASROT	identifying number of the gas rotameter
GASFLO	gas rotameter reading, %
RTCAL1	calibration constant of liquid rotameter 1 for a particular viscosity
RTCAL2	calibration constant for liquid rotameter 2
RTCAL5	calibration constant for liquid rotameter 5

For each of the RUNQTY lines, the following are then input for the  $I^{th}$  line:

LIQROT(I)	liquid rotameter identification number
LIQFLO(I)	liquid rotameter reading, %
DELHG(I)	pressure drop through valve as measured by mercury manometer, mm Hg
RMAN(I,J)	$J^{th}$ manometer reading, cm fluid

FLBD is executed after the input information from each data sheet has been accepted. The output of FLBD consists of the data sheet number, the column diameter (in.), the packing weight (gm), packing density (gm/cm<sup>3</sup>), minimum liquid fluidization velocity (cm/sec), minimum gas fluidization velocity (cm/sec), solid particle diameter (cm), liquid viscosity (poise), surface tension (dyne/cm), and for each liquid velocity the bed height (cm), pressure drop (cm fluid), gas velocity (cm/sec), liquid velocity (cm/sec), and solid, liquid, and gas holdups. The operating parameters are stored in three data files, FOR48.DAT, FOR51.DAT, and FOR54.DAT, for later use in the correlation program. Plots showing the determination of the bed height, pressure drop, and minimum fluidization velocities are output for visual inspection of the fit. Sample computer plots are shown as Figs. 23 and 24 in Sect. 8.2.5.

### 8.2.3 Computerized Determination of Bed Height, Bed Pressure Drop, and Minimum Fluidization Velocities

The pressure drop in a three-phase fluidized bed increases linearly with distance up the bed. However, in the two-phase bubble column region above the bed, the pressure drop due to flow decreases. The fluidized bed height and pressure drop across the bed can be determined from the intersection of the pressure gradients on a plot of pressure drop as a function of distance up the column. These pressure gradient lines are determined from the experimental data by locating and temporarily eliminating the input point of maximum pressure drop. Least squares lines are then fitted to the data points on either side of the maximum. The temporarily excluded point is then checked against each of the two fitted lines to determine if it lies either above the fitted line or within one standard deviation below the line. If so, the point is included in the appropriate set or sets of data for a recalculation of the least squares line. The bed height and pressure drop across the bed are then read at the point of intersection of the two lines.

A non-fluidized bed will exhibit linearly increasing bed pressure drop with an increase in the liquid velocity. However, once the minimum fluidization velocity is attained, there is no further increase in pressure drop across the bed. The liquid minimum fluidization velocity at a constant gas velocity is determined in the computer program, FLBD, from the calculated bed pressure drops and measured liquid velocities. The pressure drops, order in terms of increasing liquid velocity, are checked to determine the first local maximum pressure drop point. A least squares line is constructed through the pressure drops at liquid velocities less than and including the velocity corresponding to this first local maximum. A horizontal line is fitted to the pressure drop points at the velocities higher than this maximum. The minimum liquid fluidization velocity is then determined at the intersection of these two lines.

### 8.2.4 Listing of Data Analysis Programs

#### 8.2.4.1 FLBD.

```

REAL LIQROT, LIQFLO, MANHT3, MANHT6
DIMENSION RMAN(20, 10), MANHT3(10), MANHT6(8), PDMAX(38),
!LIQROT(20), LIQFLO(20), DELHG(20), DELTAH(19, 10), DELTH6(19, 8)
*, UG(20), EPSS(20), EPSG(20), EPSL(20), EXDATA(20, 18), VEL(20)
EQUIVALENCE(DELTAH(1, 1), DELTH6(1, 1)), (MANHT3(1), MANHT6(1))
!(LIQFLO(2), "EL(1)")
READ (10, 99) RUNQTY, DATSHT, DC, PACWT, PATM, TLIQ, "VISCOS,
!RHOG, PHOL, RHOS, SIGMA, DP, GASROT, GASFLO
VISCOS=VISCOS/100.
99  FORMAT (7E10.3)
READ (10, 98) RTCAL1, RTCAL2, RTCAL5
98  FORMAT (3E10.3)

```

```

NRUN=RUNQTY+0.001
READ (10,100) (LIQROT(I),LIQFLO(I),DELHG(I),
1(RMAN(I,J),J=1,10),I=1,NRUN)
100 FORMAT (7E10.3,/,6E10.3)
CXAREA=((DC*1.27)**2.0)*3.14159
DO 200 K=2,NRUN
J=K-1
IF (LIQROT(K)-5.) 71,70,71
71 IF (LIQROT(K)-2.) 73,72,73
73 IF (LIQROT(K)-1.) 75,74,75
70 VEL(J)=(RTCAL5*LIQFLO(K))/CXAREA
GO TO 200
72 VEL(J)=(RTCAL2*LIQFLO(K))/CXAREA
GO TO 200
74 VEL(J)=(RTCAL1*LIQFLO(K))/CXAREA
GO TO 200
75 TYPE 66, LIQROT(K)
66 FORMAT( ' ROTAMETER NUMBER L',I1, 'DOES NOT EXIST')
GO TO 10000
200 CONTINUE
IF (DC.EQ.6.) MANNO=8
IF (DC.EQ.3.) MANNO=10
DO 2 J=1,MANNO
DO 2 I=2,NRUN
IM1=I-1
2 DELTAH(IM1,J)=RMAN(I,1)-(RMAN(I,J)+RMAN(1,1)-RMAN(I,J))
NRUNM1=NRUN-1
IF (DC.EQ.3.) GO TO 3
MANHT6(1)=0.
MANHT6(2)=7.8
MANHT6(3)=16.8
MANHT6(4)=25.7
MANHT6(5)=34.7
MANHT6(6)=43.5
MANHT6(7)=52.5
MANHT6(8)=59.5
CALL POLRG (DELT6, NRUNM1, 8, MANHT6, DATSHT, PDMAX, ULMIN, VEL)
GO TO 1000
3 MANHT3(1)=1.3
MANHT3(2)=12.4
MANHT3(3)=21.4
MANHT3(4)=30.4
MANHT3(5)=43.1
MANHT3(6)=52.1
MANHT3(7)=61.1
MANHT3(8)=70.1
MANHT3(9)=79.1
MANHT3(10)=88.1
CALL POLRG (DELT6, NRUNM1, 10, MANHT3, DATSHT, PDMAX, ULMIN, VEL)
1000 IRUN=2

```

```

1 IF (GASROT-2.) 31, 32, 31
31 IF (GASROT-6.) 33, 34, 33
33 IF (GASROT-7.) 35, 36, 35
35 TYPE 67, GASROT
67 FORMAT( ' ROTAMETER NUMBER G', I1, 'DOES NOT EXIST')
GO TO 10000
32 UGCAL=(.53333*GASFLO)/CXAREA
GO TO 55
34 UGCAL=(8.5526*GASFLO)/CXAREA
GO TO 55
36 UGCAL=(93.333*GASFLO)/CXAREA
55 DELHGT=0.0
NRUN=NRUNM1+1
DO 69 K=2, NRUN
UG(K)=UGCAL*(749.8/(PATM+DELHG(K)))**.5
J=K-1
EPSS(K)=PACWT/(RHOS*CXAREA*PDMAX(J))
EPSG(K)=(RHOL-EPSS(K)*RHOL-(RHOL*(PDMAX(J)+PDMAX(J+NRUNM1))
!/PDMAX(J)))+EPSS(K)*RHOS)/(RHOL-RHOG)
EPSL(K)=1.0-EPSS(K)-EPSG(K)
IF(ULMIN.GT.VEL(J))IRUN=K+1
97 DELHGT=DELHGT+DELHG(K)
69 CONTINUE
DELHGA=DELHGT/NRUNM1
UGAVG=UGCAL*(749.8/(PATM+DELHGA))**.5
IDATST=DATSHT+0.001
TYPE 101, IDATST, DC, PACWT, RHOS, ULMIN, UGAVG, DP, VISCOS, SIGMA
101 FORMAT(10X, 'DATA SHEET #', I3,/, 10X, 'COLUMN DIAMETER =',
!F4.2, ' INCHES',/, 10X, 'PACKING WEIGHT =', F8.0, ' GRAMS',/,
!10X, 'PACKING DENSITY =', F8.2, ' GRAMS/CC',/, 10X,
! 'UL MINIMUM =', F7.2, ' CM/SEC',/, 10X, 'UG MINIMUM =',
!F7.2, ' CM/SEC',/, 10X, 'PARTICLE DIAMETER =', F7.3,
! ' CM',/, 10X, 'VISCOSITY = ', F7.4, ' POISE',/, 10X,
! 'SURFACE TENSION = ', F5.1, ' DYNES/CM')
TYPE 2050
2050 FORMAT(' BED HT    DEL PRES     UG        UL      EPS SOLID',
! ' EPS LIQ    EPS GAS')
DO 2080 K=2, NRUN
J=K-1
2080 TYPE 2075, PDMAX(J), PDMAX(J+NRUNM1), UG(K),
!VEL(J), EPSS(K), EPSL(K), EPSG(K)
2075 FORMAT(7E10.3)
DO 156 K=IRUN, NRUN
J=K-1
EXDATA(K, 1)=UG(K)
EXDATA(K, 2)=VEL(J)
EXDATA(K, 3)=DP
EXDATA(K, 4)=RHOS
EXDATA(K, 5)=RHOL
EXDATA(K, 6)=RHOG
EXDATA(K, 7)=SIGMA

```

```

EXDATA(K,8)=VI SCOS
EXDATA(K,9)=EPSS(K)
EXDATA(K,10)=1.-EPSS(K)
EXDATA(K,11)=EPSG(K)
EXDATA(K,12)=EPSL(K)
EXDATA(K,13)=DC*2.54
EXDATA(K,14)=PDMAX(J)
EXDATA(K,15)=PDMAX(J+NRUNM1)
EXDATA(K,16)=UGAVG
EXDATA(K,17)=ULMIN
EXDATA(K,18)=DATSHT
156  CONTINUE
      TYPE 102
102  FORMAT(//, IX, 'IF YOU WANT THIS INFORMATION
      ! STORED ON FILES 48, 51 & 54 TYPE Y,<CR>')
      ACCEPT 103, ISTR
103  FORMAT(A5)
      IF (ISTR.NE.'Y') GO TO 10000
      OPEN(UNIT=48, ACCESS= 'APPEND')
      WRITE(48,104)((EXDATA(I,J),J=1,6),I=IRUN,NRUN)
      OPEN(UNIT=51, ACCESS= 'APPEND')
      WRITE(51,104)((EXDATA(I,J),J=7,12),I=IRUN,NRUN)
      OPEN(UNIT=54, ACCESS= 'APPEND')
      WRITE(54,104)((EXDATA(I,J),J=13,18),I=IRUN,NRUN)
104  FORMAT(6E10.3)
10000 CALL EXIT
      END

```

#### 8.2.4.2 POLRG

```

SUBROUTINE POLRG(DELTAH,NRUNM1,N,MANHT,DATSHT,PDMAX,ULMIN,VEL)
REAL MANHT(1)
DIMENSION DELTAH(1),PDMAX(38),Y(20),X(96)
C MANHT=POSITIONS UP COLUMN, NRUNM1=NUM.OF RUNS ON DATA SHT
C N=NUMBER OF MANS., DELTAH=PRESS DROP VALUES
C OUTPUT: PDMAX(NRUNM1+1:2NRUNM1)=MAX PRESS DROP PER RUN
C          PDMAX(1:NRUNM1)=HT UP COLUMN AT PDMAX(,2)'S
DIMENSION B(7),E(7),SB(7),T(7),DI(49),D(36)
DIMENSION XBAR(8),STD(8),COE(8),SUMSQ(8),ISAVE(8)
DIMENSION ANS(10),A(5000),VEL(1)
CALL PLOTS(A,5000)
LOOP=0
600 LOOP=LOOP+1
620 CALL PLOT(1.5,1.5,3)
      CALL PLOT(1.5,7.5,2)
      CALL PLOT(9.6,7.5,1)
      CALL PLOT(9.6,1.5,1)
      CALL PLOT(1.5,1.5,1)

```

```

X1=1.5
Y1=1.5
DO 50 J=1,8
X1=X1+0.9
50 CALL SYMBOL(X1,Y1,0.125,13,0.0,-1)
CALL PLOT(1.5,1.5,3)
X1=1.5
DO 70 J=1,5
Y1=Y1+1.0
70 CALL SYMBOL(X1,Y1,0.125,15,0.0,-1)
M=1
MM=2
L=N*M
DO 110 I=1,N
J=L+I
C X(I) IS INDEPENDENT VARIABLE,X(J) IS DEPENDENT. FROM FLBED1
X(I)=MANHT(I)
110 X(J)=DELTAH(19*(I-1)+LOOP)
XHIGH=90.0
XLOW=0.0
YHIGH=25.0
YLOW=-5.0
IPEAK=L+1
DO 300 I =1,N
J=L+I
IF(X(J).GT.X(IPEAK))IPEAK=J
300 CONTINUE
IPEAK=IPEAK-L
DELX=XHIGH-0.0
IF(IPEAK.LT.3)GO TO 610
IF (IPEAK.GT.N-3)GO TO 610
92 FORMAT(1X,2E10.3)
IPASS=0
IFLAG=0
LIM=IPEAK+1
LIMIT=IPEAK-1
960 DO 700 I=1,LIMIT
Y(I)=X(I)
J=LIMIT+I
700 Y(J)=X(L+I)
705 CALL CORREC(LIMIT,MM,1,Y,XBAR,STD,COE,D,SUMSQ,B,T)
NT=LIMIT-1
ISAVE(1)=1
CALL ORDER(MM,D,MM,M,ISAVE,DI,E)
CALL MINV(DI,M,DET,B,T)
CALL MULTR(LIMIT,M,XBAR,STD,SUMSQ,DI,E,ISAVE,B,SB,T,ANS)
NI=ANS(8)
COE(1)=ANS(1)
COE(2)=B(1)
SUMIP=0.0
LA=1

```

```

      IF(IFLAG.GT.0)GO TO 953
950 LIMIT=LIMIT+1
      IFLAG=1
      GO TO 960
610 DO 650 I=LOOP,NRUNM1
      VEL(I)=VEL(I+1)
      DELTAH(I)=DELTAH(I+1)
650 PDMAX(I)=PDMAX(I+1)
      NNEW=(NRUNM1-1)*2
      DO 660 I=NRUNM1,NNEW
      PDMAX(I)=PDMAX(I+1)
660 IF(I.GE.LOOP) PDMAX(I)=PDMAX(I+1)
      NRUNM1=NRUNM1-1
      TYPE 670, DATSHT
670 FORMAT (' ONE LINE DELETED FROM DATA SHEET #',F4.0)
      IF (LOOP.GT.NRUNM1)GO TO 680
      GO TO 620
953 CONTINUE
      IF(IPASS.GT.0)GO TO 990
      FINTER=COE(1)
      FSLOPE=COE(2)
715 IFLAG=0
980 J=0
      DO 710 I=LIM,N
      J=J+1
      Y(J)=X(I)
      JJJ=N-LIM+1+J
710 Y(JJJ)=X(L+I)
      IPASS=1
      LIMIT=N-LIM+1
      CALL CORRE(LIMIT,MM,1,Y,XBAR,STD,COE,D,SUMSQ,B,T)
      NT=LIMIT-1
      ISAVE(1)=1
      CALL ORDER(MM,D,MM,M,ISAVE,DI,E)
      CALL MINV(DI,M,DET,B,T)
      CALL MULTR(LIMIT,M,XBAR,STD,SUMSQ,DI,E,ISAVE,B,SB,T,ANS)
      NI=ANS(8)
      COE(1)=ANS(1)
      COE(2)=B(1)
      SUMIP=0.0
      LA=1
      IF(IFLAG.GT.0)GO TO 953
      IF(X(L+IPEAK).LT.X(IPEAK)*COE(2)+COE(1))GO TO 1051
970 LIM=LIM-1
      IFLAG=1
      LIMIT=LIMIT+1
      IPASS=0
      GO TO 980
1051 IF(X(IPEAK)*COE(2)+COE(1)-STD(1).GT.X(L+IPEAK))GO TO 953
      GO TO 970

```

```

C HAVE SOLVED FOR BOTH SLOPES AND INTERCEPTS
C SOLVE FOR INTERSECTION
990 XINTER=(COE(1)-FINTER)/(FSLOPE-COE(2))
YINTER=FINTER+FSLOPE*XINTER
IF(YINTER.GT.25)GO TO 800
DELY=30.
YCURV=(FINTER-YLOW)/DELY*6.0+1.5
CALL PLOT(1.5,YCURV,3)
C PLOT LINES
XCURV=(XINTER-XLOW)/DELX*8.1+1.5
YCURV=(YINTER-YLOW)/DELY*6.0+1.5
CALL PLOT(XCURV,YCURV,2)
XCURV=8.1+1.5
YCURV=(COE(1)+COE(2)*90.-YLOW)/DELY*6.0+1.5
CALL PLOT(XCURV,YCURV,2)
DO 90 I=1,N
J=L+I
XPOINT=(X(I)-XLOW)/DELX*8.1+1.5
YPOINT=(X(J)-YLOW)/DELY*6.0+1.5
90 CALL SYMBOL(XPOINT,YPOINT,0.2,2,0.0,-1)
800 PDMAX(LOOP)=XINTER
IDUMMY=NRUNM1+LOOP
PDMAX(IDUMMY)=YINTER
680 CALL NUMBER(0.5,0.5,0.4,DATSHT,0.0,*(F4.0)*,4)
CALL PLOT(14.,0.0,3)
C ADVANCE TO NEW GRAPH
CALL PLOT(14.,0.0,-3)
IF (LOOP.LT.NRUNM1)GO TO 600
CALL LFMIN(NRUNM1,PDMAX,VEL,ULMIN,PDPMIN,DATSHT)
RETURN
END

```

#### 8.2.4.3 LFMIN.

```

SUBROUTINE LFMIN(N,X,VEL,XINT,YINT,DATSHT)
DIMENSION X(1),Y(100),VEL(1),YBAR2(8),STD2(8),
*D(36),SUMSQ(8),ISAVE(8),ANS(10),DI(49),RX1(8),D1(7)
*,B1(8),STD1(8),YBAR1(8),T1(7),R1(36),E(7),B(7),SB(7),T(7)
C N=NUMBER OF OBSERVATIONS
C VEL HAS LIQ VELOCITIES. X HAS HTS.,PRESS DROPS
C THIS ROUTINE CALLS GDATA,ORDER,MINV,MULTR,CORRE
C XINT=MIN. LIQ. FLUIDIZATION VEL.;YINT=PRESS DROP
DO 100 I=2,N
JSAVE=I-1
100 IF(X(N+I).LT.X(N+JSAVE))GOTO 200
C LAST X IS LARGEST IN ALWAYS INCREASING PATTERN
TYPE 101
101 FORMAT(' NO STOP IN RISE, DATA NEVER FLUIDIZED!')
XINT=VEL(N)*1.1
YINT=X(N)*1.1
RETURN

```

```

C X(JSAVE) IS LOCAL PEAK
200 NUMBER=N-JSAVE
    IF(NUMBER.LE.2) GO TO 300
    DO 201 I=1,NUMBER
    J=N+JSIZE+I
201 Y(I)=X(J)
    CALL CORRE(NUMBER, 1, 1, Y, YBAR1, STD1, RX1, R1, B1, D1, T1)
    DO 203 I=1,NUMBER
    NUM=NUMBER+I
    Y(I)=VEL(JSAVE+I)
203 Y(NUM)=X(N+JSIZE+I)
    CALL GDATA(NUMBER, 1, Y, YBAR2, STD2, D, SUMSQ)
    ISAVE(1)=1
    CALL ORDER(2, D, 2, 1, ISAVE, DI, E)
    CALL MINV(DI, 1, DET, B, T)
    CALL MULTR(NUMBER, 1, YBAR2, STD2, SUMSQ, DI, E, ISAVE, B, SB, T, ANS)
    FSLOPE=B(1)
    FINTER=ANS(1)
C NOW PROCESS POINTS WHICH WERE NOT USED
    IF(JSIZE.LE.2)GO TO 302
    DO 210 I=1,JSIZE
    J=JSIZE+I
    Y(I)=VEL(I)
210 Y(J)=X(N+I)
    CALL GDATA(JSIZE, 1, Y, YBAR2, STD2, D, SUMSQ)
    ISAVE(1)=1
    CALL ORDER(2, D, 2, 1, ISAVE, DI, E)
    CALL MINV(DI, 1, DET, B, T)
    CALL MULTR(JSIZE, 1, YBAR2, STD2, SUMSQ, DI, E, ISAVE, B, SB, T, ANS)
    ANSWER=ANS(1)
    GO TO 400
300 TYPE 301,NUMBER
301 FORMAT(' ONLY',I4,' POINTS FOR CORRE. STOP')
    RETURN
302 TYPE 303,JSIZE
303 FORMAT(' ONLY',I4,' POINTS FOR UNDER FL. LINE')
    RETURN
400 XINT=(YBAR1(1)-ANS(1))/B(1)
    YINT=YBAR1(1)
    CALL UPLDT(XINT,YINT,ANSWER,B,FINTER,FSLOPE,N,X,VEL,DATSHT)
    RETURN
    END

```

8.2.4.4 UPLOT.

```

SUBROUTINE UPLOT(XINT,YINT,ANSWER,B,FINTER,FSLOPE,N,X,VEL,DATA)
C   PLOTTING FOR SUBROUTINE ULMIN
  DIMENSION X(1),VEL(1),Y(100)
  DELX=10.0/8.
  DELY=30./6.
  CALL PLOT(1.5,1.5,3)
  CALL PLOT(1.5,7.5,2)
  CALL PLOT(9.5,7.5,1)
  CALL PLOT(9.5,1.5,1)
  CALL PLOT(1.5,1.5,1)
  X1=1.5
  Y1=1.5
  DO 500 J=1,9
  X1=X1+0.8
500 CALL SYMBOL(X1,Y1,0.125,13,0.0,-1)
  CALL PLOT(1.5,1.5,3)
  X1=1.5
  DO 501 J=1,5
  Y1=Y1+1.0
501 CALL SYMBOL(X1,Y1,0.125,15,0.0,-1)
  CALL PLOT(1.5,7.5,3)
  Y1=7.5
  DO 502 J=1,9
  X1=X1+0.8
502 CALL SYMBOL(X1,Y1,0.125,13,180.0,-1)
  CALL PLOT(9.5,1.5,3)
  X1=9.5
  Y1=1.5
  DO 503 J=1,5
  Y1=Y1+1.0
503 CALL SYMBOL(X1,Y1,0.125,15,180.0,-1)
C   PLOTS LINE
  IF(YINT.LE.0.) GO TO 600
  XPT=XINT/DELX+1.5
  YPT=YINT/DELY+1.5
  TYPE 8002,XPT,YPT
8002 FORMAT(' HORIZ LINE= ',2E10.3)
  CALL PLOT(XPT,YPT,3)
  CALL PLOT(9.5,YPT,2)
  TYPE 8003,YPT
8003 FORMAT(' TO 9.5 ',E10.3)
C   PLOT ST. LINE FOR UNDER FLUIDIZATION
  FPT=ANSWER/DELY+1.5
  CALL PLOT(1.5,FPT,3)
  TYPE 8005,XPT,YPT
8005 FORMAT(' INTERSECT= ',2E10.3)
  CALL PLOT(XPT,YPT,2)
C   PLOT ACTUAL LINE OF BEST FIT OF R.H.S.

```

```

XPT=(FINTER-ANSWER)/(B-F SLOPE)
YPT=(B*XPT+ANSWER)/DELY+1.5
XPT=XPT/DELX+1.5
CALL PLOT(XPT,YPT,3)
XPT=10.
YPT=(FSLOPE*XPT+FINTER)/DELY+1.5
XPT=10./DELX+1.5
CALL PLOT(XPT,YPT,2)
C NOW PLOT EXP POINTS
C POINTS ARE IN[Y(I),Y(N+I)] PAIRS
DO 510 I=1,N
J=N+I
Y(I)=VEL(I)
510 Y(J)=X(J)
DO 511 I=1,N
J=N+I
XPT=Y(I)/DELX+1.5
YPT=Y(J)/DELY+1.5
511 CALL SYMBOL(XPT,YPT,0.2,2,0.0,-1)
CALL NUMBER(0.5,0.5,0.4,DATSH,0.0, "(F4.0)",4)
600 CALL PLOT(14.,0.0,-3)
RETURN
END

```

#### 8.2.4.5 EXPINP.

```

REAL LIQROT,LIQFLO
DIMENSION RMAN(20,10),LIQROT(20),LIQFLO(20),DELHG(20)
ACCEPT 100, RUNQTY,DATSH,DC,PACWT,PATM,TLIQ,VISCOS,RHOG,
!RHOL,RHOS,SIGMA,DP,GASROT,GASFLO,RTCAL1,RTCAL2,RTCAL5
100 FORMAT (17G)
NRUN=RUNQTY
DO 1 I=1,NRUN
ACCEPT 101,LIQROT(I),LIQFLO(I),DELHG(I),(RMAN(I,J),J=1,10)
101 FORMAT (13G)
1 CONTINUE
OPEN (UNIT=10,ACCESS="APPEND")
WRITE (10,103) RUNQTY,DATSH,DC,PACWT,PATM,TLIQ,VISCOS,
!RHOG,RHOL,RHOS,SIGMA,DP,GASROT,GASFLO
103 FORMAT (7E10.3)
WRITE (10,107) RTCAL1,RTCAL2,RTCAL5
107 FORMAT (3E10.3)
WRITE (10,104) (LIQROT(I),
!LIQFLO(I),DELHG(I),(RMAN(I,J),J=1,10),I=1,NRUN)
104 FORMAT (7E10.3,/,6E10.3)
TYPE 106, RUNQTY,DATSH,DC,PACWT,PATM,TLIQ,VISCOS,
!RHOG,RHOL,RHOS,SIGMA,DP,GASROT,GASFLO
106 FORMAT (///,(7E10.3))
TYPE 108, RTCAL1,RTCAL2,RTCAL5
108 FORMAT (///,3E10.3)

```

```

      TYPE 105, (LIQROT(I),
      !LIQFLO(I),DELHG(I),(RMAN(I,J),J=1,10),I=1,NRUN)
105  FORMAT (//,7E10.3,/,6E10.3)
      CALL EXIT
      END

```

### 8.2.5 Sample Output

```

0.150E+02 0.900E+01 0.300E+01 0.250E+04 0.747E+03 0.231E+02 0.900E+00
0.130E-02 0.996E+00 0.226E+01 0.712E+02 0.462E+00 0.600E+01 0.800E+02
0.544E+01 0.278E+01 0.279E+01
0.500E+01 0.000E+00 0.700E+01 0.476E+02 0.477E+02 0.477E+02 0.476E+02
0.476E+02 0.474E+02 0.477E+02 0.476E+02 0.477E+02 0.478E+02
0.500E+01 0.120E+02 0.100E+03 0.425E+02 0.411E+02 0.385E+02 0.358E+02
0.340E+02 0.354E+02 0.373E+02 0.395E+02 0.415E+02 0.436E+02
0.500E+01 0.160E+02 0.101E+03 0.480E+02 0.444E+02 0.407E+02 0.372E+02
0.341E+02 0.358E+02 0.377E+02 0.398E+02 0.417E+02 0.443E+02
0.500E+01 0.240E+02 0.105E+03 0.554E+02 0.486E+02 0.440E+02 0.390E+02
0.351E+02 0.361E+02 0.384E+02 0.402E+02 0.421E+02 0.444E+02
0.500E+01 0.320E+02 0.105E+03 0.569E+02 0.498E+02 0.448E+02 0.406E+02
0.351E+02 0.360E+02 0.382E+02 0.404E+02 0.424E+02 0.448E+02
0.500E+01 0.400E+02 0.105E+03 0.579E+02 0.504E+02 0.458E+02 0.417E+02
0.364E+02 0.365E+02 0.386E+02 0.407E+02 0.429E+02 0.450E+02
0.500E+01 0.480E+02 0.105E+03 0.590E+02 0.513E+02 0.468E+02 0.432E+02
0.373E+02 0.371E+02 0.390E+02 0.407E+02 0.426E+02 0.451E+02
0.500E+01 0.560E+02 0.107E+03 0.590E+02 0.525E+02 0.472E+02 0.439E+02
0.380E+02 0.366E+02 0.389E+02 0.409E+02 0.428E+02 0.452E+02
0.100E+01 0.300E+02 0.107E+03 0.595E+02 0.534E+02 0.483E+02 0.446E+02
0.384E+02 0.372E+02 0.390E+02 0.411E+02 0.428E+02 0.451E+02
0.100E+01 0.350E+02 0.108E+03 0.604E+02 0.544E+02 0.494E+02 0.454E+02
0.393E+02 0.379E+02 0.396E+02 0.416E+02 0.434E+02 0.458E+02
0.100E+01 0.400E+02 0.108E+03 0.612E+02 0.554E+02 0.504E+02 0.465E+02
0.401E+02 0.384E+02 0.398E+02 0.418E+02 0.436E+02 0.457E+02
0.100E+01 0.450E+02 0.109E+03 0.622E+02 0.560E+02 0.512E+02 0.478E+02
0.416E+02 0.394E+02 0.403E+02 0.421E+02 0.441E+02 0.462E+02
0.100E+01 0.500E+02 0.109E+03 0.629E+02 0.567E+02 0.520E+02 0.485E+02
0.422E+02 0.401E+02 0.409E+02 0.424E+02 0.444E+02 0.465E+02
0.100E+01 0.600E+02 0.110E+03 0.635E+02 0.580E+02 0.536E+02 0.510E+02
0.448E+02 0.419E+02 0.419E+02 0.432E+02 0.450E+02 0.471E+02
0.100E+01 0.700E+02 0.110E+03 0.639E+02 0.590E+02 0.552E+02 0.530E+02
0.478E+02 0.446E+02 0.436E+02 0.440E+02 0.452E+02 0.476E+02

```

```
•EX FLBD,LIBRARY, SYS: PLOT/SEA

LINK:    LOADING
[LNKXCT FLBD EXECUTION]

!SAVE THIS PLOT? Y FOR YES

Y
!SAVED PLOT  1
!SAVE THIS PLOT? Y FOR YES

Y
!SAVED PLOT  2
!SAVE THIS PLOT? Y FOR YES

Y
!SAVED PLOT  3
!SAVE THIS PLOT? Y FOR YES

Y
!SAVED PLOT  4
!SAVE THIS PLOT? Y FOR YES

Y
!SAVED PLOT  5
!SAVE THIS PLOT? Y FOR YES

Y
!SAVED PLOT  6
!SAVE THIS PLOT? Y FOR YES

Y
!SAVED PLOT  7
!SAVE THIS PLOT? Y FOR YES

Y
!SAVED PLOT  8
!SAVE THIS PLOT? Y FOR YES

Y
!SAVED PLOT  9
!SAVE THIS PLOT? Y FOR YES

Y
!SAVED PLOT 10
!SAVE THIS PLOT? Y FOR YES

Y
!SAVED PLOT 11
!SAVE THIS PLOT? Y FOR YES
```

```

Y
!SAVED PLOT 12
!SAVE THIS PLOT? Y FOR YES

Y
!SAVED PLOT 13
!SAVE THIS PLOT? Y FOR YES

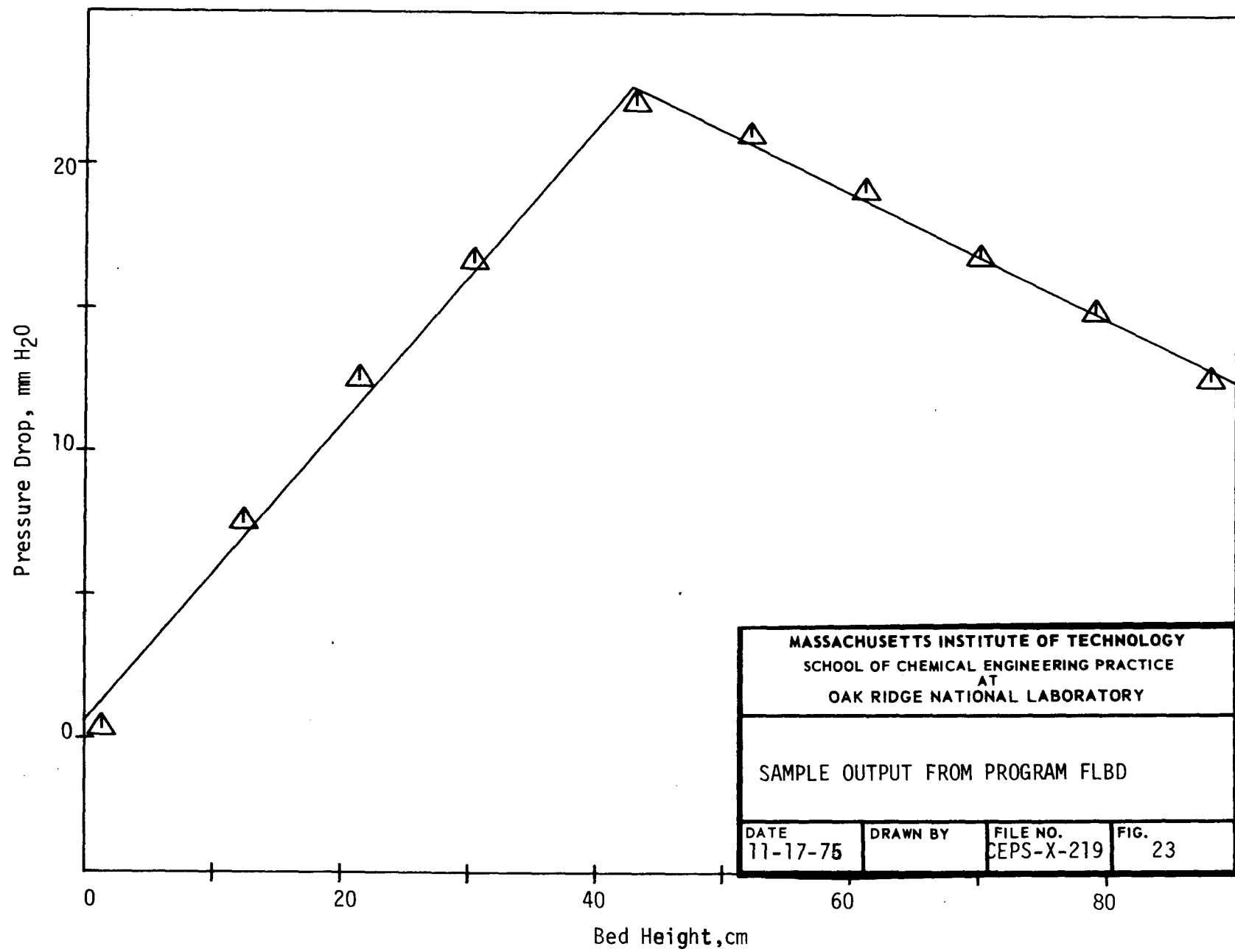
Y
!SAVED PLOT 14
HORIZ LINE= 0.297E+01 0.604E+01
TO 9.5 0.604E+01
INTERSECT= 0.297E+01 0.604E+01
!SAVE THIS PLOT? Y FOR YES

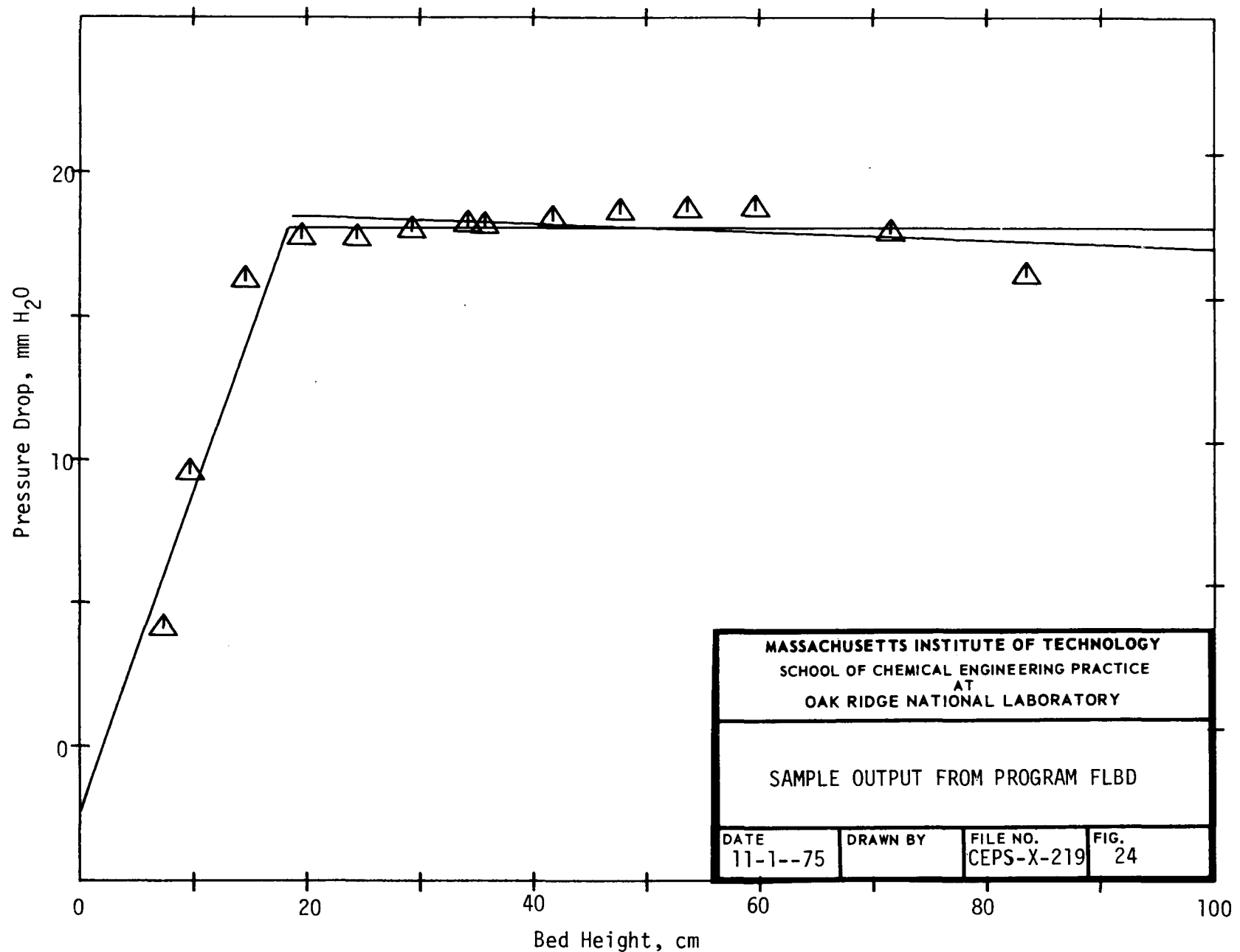
Y
!SAVED PLOT 15
  DATA SHEET # 9
  COLUMN DIAMETER = 3.00 INCHES
  PACKING WEIGHT = 2500. GRAMS
  PACKING DENSITY = 2.26 GRAMS/CC
  UL MINIMUM = 1.84 CM/SEC
  UG MINIMUM = 14.06 CM/SEC
  PARTICLE DIAMETER = 0.462 CM
  VISCOSITY = 0.0090 POISE
  SURFACE TENSION = 71.2 DYNES/CM
  BED HT    DEL PRES      UG      UL      EPS SOLID    EPS LIQ    EPS GAS
0.430E+02 0.877E+01 0.141E+02 0.734E+00 0.564E+00-0.769E-01 0.513E+00
0.424E+02 0.142E+02 0.141E+02 0.979E+00 0.572E+00 0.363E-01 0.391E+00
0.419E+02 0.209E+02 0.141E+02 0.147E+01 0.579E+00 0.185E+00 0.236E+00
0.428E+02 0.224E+02 0.141E+02 0.196E+01 0.567E+00 0.236E+00 0.197E+00
0.432E+02 0.224E+02 0.141E+02 0.245E+01 0.562E+00 0.243E+00 0.195E+00
0.485E+02 0.226E+02 0.141E+02 0.294E+01 0.500E+00 0.332E+00 0.168E+00
0.494E+02 0.228E+02 0.141E+02 0.343E+01 0.491E+00 0.348E+00 0.161E+00
0.496E+02 0.228E+02 0.141E+02 0.358E+01 0.489E+00 0.349E+00 0.161E+00
0.498E+02 0.230E+02 0.141E+02 0.418E+01 0.487E+00 0.357E+00 0.156E+00
0.502E+02 0.233E+02 0.141E+02 0.477E+01 0.483E+00 0.367E+00 0.150E+00
0.510E+02 0.233E+02 0.140E+02 0.537E+01 0.476E+00 0.378E+00 0.146E+00
0.510E+02 0.234E+02 0.140E+02 0.596E+01 0.476E+00 0.378E+00 0.146E+00
0.574E+02 0.225E+02 0.140E+02 0.716E+01 0.422E+00 0.434E+00 0.144E+00
0.594E+02 0.211E+02 0.140E+02 0.835E+01 0.408E+00 0.428E+00 0.164E+00

```

IF YOU WANT THIS INFORMATION STORED ON FILES 48, 51 & 54 TYPE Y,<CR>  
N

END OF EXECUTION





MASSACHUSETTS INSTITUTE OF TECHNOLOGY  
SCHOOL OF CHEMICAL ENGINEERING PRACTICE  
AT  
OAK RIDGE NATIONAL LABORATORY

SAMPLE OUTPUT FROM PROGRAM FLBD

DATE 11-1--75 DRAWN BY FILE NO. CEPS-X-219 FIG. 24

### 8.3 Correlation Program

#### 8.3.1 Explanation of CORRLT

This correlation program performs correlations of the form:

$$Z = e^{K a B^b C^c} \dots \quad (23)$$

for up to thirteen independent variables and two thousand data points. The user selects the variables desired for correlation from a list of twenty-eight available, including both dimensional and dimensionless operating parameters. The program reads the appropriate literature and experimental, dimensional, and dimensionless data files designated by the user. Any lines of data containing zero or negative data intended for the correlation are deleted. Natural logs of all remaining data are calculated and the resulting array is sent to the IBM Scientific Subroutines of CORRE, ORDER, MINU, and MULTR for linear regression analysis.

#### 8.3.2 CORRLT Input and Output

Prior to execution of CORRLT, data files FOR48.DAT, FOR51.DAT, and FOR54.DAT, containing the experimental operating parameters, must be in the disk space. If correlations are to be performed using literature points, files FOR30.DAT and FOR32.DAT must be present. If dimensionless groups are to be correlated, files FOR33.DAT and FOR45.DAT, as calculated by computer DIMLES, are required. In the execution of CORRLT, the desired variables, up to a maximum of fourteen, are selected by assigning sequential item numbers to the variables as requested by the program. A definition of each of these variables is found in the program DIMLES. Other input includes the total number of the variables correlated, the designation of the dependent variable by its item number, and the number of lines of experimental and literature data available for correlation.

CORRLT performs a linear regression on the variables selected. The output includes the regression coefficients, or the exponents in Eq. (23), the intercept K, in Eq. (23), and the statistical parameters characterizing the significance of these values and of the obtained correlation. The output also includes a list comparing the experimental and calculated values of the dependent variable from the correlation. A plot of this comparison, may be obtained from subroutine DECWAR if desired.

8.3.3 Listing of Correlation Programs8.3.3.1 CORRLT.

```

INTEGER ENDEXP, BGNLIT, ENDLIT, ENDALL, DEPEN
DIMENSION DIMEN(2000,15), AUTH(2000), X(28000), XBAR(15),
!SB(14), ANS(10), STD(15), RX(225), RY(14), B(15), D(15), T(15),
!FINAL(2000,2), ISAVE(15), R(225)
EQUIVALENCE (DIMEN(1,15), AUTH(1)), (DIMEN(1,1), X(1))
DATA J1,J2,J3,J4,J5,J6,J7,J8,J9,J10,J11,J12,J13,J14,
!K1,K2,K3,K4,K5,K6,K7,K8,K9,K10,K11,K12,K13,K14/28*15/
TYPE 300
300  FORMAT (* IF YOU WANT A LIST OF CORRELATION OPTIONS, *,
!*TYPE 1 <CR>. ELSE TYPE 2 <CR>)
ACCEPT *, L0
TYPE 305
ACCEPT *, L1
GO TO (10,14), L0
10  GO TO (11,12,11), L1
11  TYPE 100
TYPE 101
ACCEPT *, J1
TYPE 102
ACCEPT *, J2
TYPE 103
ACCEPT *, J3
TYPE 104
ACCEPT *, J4
TYPE 105
ACCEPT *, J5
TYPE 106
ACCEPT *, J6
TYPE 107
ACCEPT *, J7
TYPE 108
ACCEPT *, J8
TYPE 113
ACCEPT *, J13
TYPE 114
ACCEPT *, J14
12  TYPE 109
ACCEPT *, J9
TYPE 110
ACCEPT *, J10
TYPE 111
ACCEPT *, J11
TYPE 112
ACCEPT *, J12
GO TO (18,13,13), L1

```

13     TYPE 201  
      ACCEPT \*, K1  
      TYPE 202  
      ACCEPT \*, K2  
      TYPE 203  
      ACCEPT \*, K3  
      TYPE 204  
      ACCEPT \*, K4  
      TYPE 205  
      ACCEPT \*, K5  
      TYPE 206  
      ACCEPT \*, K6  
      TYPE 207  
      ACCEPT \*, K7  
      TYPE 208  
      ACCEPT \*, K8  
      TYPE 209  
      ACCEPT \*, K9  
      TYPE 210  
      ACCEPT \*, K10  
      TYPE 211  
      ACCEPT \*, K11  
      TYPE 212  
      ACCEPT \*, K12  
      TYPE 213  
      ACCEPT \*, K13  
      TYPE 214  
      ACCEPT \*, K14  
      GO TO 18  
14     GO TO (15,16,15), L1  
15     ACCEPT \*, J1  
      ACCEPT \*, J2  
      ACCEPT \*, J3  
      ACCEPT \*, J4  
      ACCEPT \*, J5  
      ACCEPT \*, J6  
      ACCEPT \*, J7  
      ACCEPT \*, J8  
      ACCEPT \*, J13  
      ACCEPT \*, J14  
16     ACCEPT \*, J9  
      ACCEPT \*, J10  
      ACCEPT \*, J11  
      ACCEPT \*, J12  
      GO TO (18,17,17), L1  
17     ACCEPT \*, K1  
      ACCEPT \*, K2  
      ACCEPT \*, K3  
      ACCEPT \*, K4  
      ACCEPT \*, K5

```

ACCEPT *, K6
ACCEPT *, K7
ACCEPT *, K8
ACCEPT *, K9
ACCEPT *, K10
ACCEPT *, K11
ACCEPT *, K12
ACCEPT *, K13
ACCEPT *, K14
18  TYPE 301
ACCEPT *, NOVAR
TYPE 302
ACCEPT *, DEPEN
TYPE 303
ACCEPT *, ENDEXP
TYPE 304
ACCEPT *, ENDIT
100 FORMAT(//, ' YOU HAVE A CHOICE OF CORRELATING 14 OR LESS '.
!, 'VARIABLES.', /)
101 FORMAT(' TO CORRELATE   UG : TYPE ITEM#. ELSE 15 <CR> #')
102 FORMAT(' TO CORRELATE   UL : TYPE ITEM#. ELSE 15 <CR> #")
103 FORMAT(' TO CORRELATE   DP : TYPE ITEM#. ELSE 15 <CR> #")
104 FORMAT(' TO CORRELATE   RHOS : TYPE ITEM#. ELSE 15 <CR> #")
105 FORMAT(' TO CORRELATE   RHOL : TYPE ITEM#. ELSE 15 <CR> #")
106 FORMAT(' TO CORRELATE   RHOG : TYPE ITEM#. ELSE 15 <CR> #")
107 FORMAT(' TO CORRELATE   SIGMA: TYPE ITEM#. ELSE 15 <CR> #")
108 FORMAT(' TO CORRELATE   VISCOS: TYPE ITEM#. ELSE 15 <CR> #")
113 FORMAT(' TO CORRELATE   DC : TYPE ITEM#. ELSE 15 <CR> #")
114 FORMAT(' TO CORRELATE   ULMIN: TYPE ITEM#. ELSE 15 <CR> #")
109 FORMAT(' TO CORRELATE   EPSS : TYPE ITEM#. ELSE 15 <CR> #")
110 FORMAT(' TO CORRELATE   1-EPSS: TYPE ITEM#. ELSE 15 <CR> #")
111 FORMAT(' TO CORRELATE   EPSG : TYPE ITEM#. ELSE 15 <CR> #")
112 FORMAT(' TO CORRELATE   EPSL : TYPE ITEM#. ELSE 15 <CR> #")
201 FORMAT(' TO CORRELATE   WEL : TYPE ITEM#. ELSE 15 <CR> #")
202 FORMAT(' TO CORRELATE   WEG : TYPE ITEM#. ELSE 15 <CR> #")
203 FORMAT(' TO CORRELATE   FRG : TYPE ITEM#. ELSE 15 <CR> #")
204 FORMAT(' TO CORRELATE   FRL : TYPE ITEM#. ELSE 15 <CR> #")
205 FORMAT(' TO CORRELATE   REL : TYPE ITEM#. ELSE 15 <CR> #")
206 FORMAT(' TO CORRELATE   REG : TYPE ITEM#. ELSE 15 <CR> #")
207 FORMAT(' TO CORRELATE   UG/UL : TYPE ITEM#. ELSE 15 <CR> #")
208 FORMAT(' TO CORRELATE   DC/DP : TYPE ITEM#. ELSE 15 <CR> #")
209 FORMAT(' TO CORRELATE   GA : TYPE ITEM#. ELSE 15 <CR> #")
210 FORMAT(' TO CORRELATE   ORNL : TYPE ITEM#. ELSE 15 <CR> #")
211 FORMAT(' TO CORRELATE   BO : TYPE ITEM#. ELSE 15 <CR> #")
212 FORMAT(' TO CORRELATE   AR : TYPE ITEM#. ELSE 15 <CR> #")
213 FORMAT(' TO CORRELATE   CA : TYPE ITEM#. ELSE 15 <CR> #")
214 FORMAT(' TO CORRELATE   CD : TYPE ITEM#. ELSE 15 <CR> #")
301 FORMAT (' THE NUMBER OF VARIABLES CHOSEN = ')
302 FORMAT (' THE ITEM NUMBER OF THE DEPENDENT VARIABLE = ')
303 FORMAT (' THE NUMBER OF LINES OF EXPERIMENTAL INPUT = ')

```

```

304  FORMAT (' THE NUMBER OF LINES OF LITERATURE INPUT = ')
305  FORMAT (' TYPE 1 <CR> FOR DIMENSIONAL GROUPS ONLY',/,'
! TYPE 2 <CR> FOR DIMENSIONLESS GROUPS ONLY',/,'
! TYPE 3 <CR> FOR BOTH DIMENSIONAL AND NONDIMENSIONAL ')
    TYPE 5000,J1,J2,J3,J4,J5,J6,J7,J8,J9,J10,J11,J12,J13,J14,
!K1,K2,K3,K4,K5,K6,K7,K8,K9,K10,K11,K12,K13,K14,NOVAR,
!DEPEN,ENDEXP,ENDLIT
5000  FORMAT (24I3,/,8I5,/)
    DO 22 I=1,ENDEXP
    IF (L1.EQ.1) GO TO 21
    READ (33,402) DIMEN(I,K1),DIMEN(I,K2),DIMEN(I,K3),
!DIMEN(I,K4),DIMEN(I,K5),DIMEN(I,K6),DIMEN(I,K7),
!DIMEN(I,K8),DIMEN(I,K9),DIMEN(I,K10),DIMEN(I,K11),
!DIMEN(I,K12),DIMEN(I,K13),DIMEN(I,K14)
402   FORMAT (14E10.3)
21    READ (48,401) (DIMEN(I,J1),DIMEN(I,J2),DIMEN(I,J3),
!DIMEN(I,J4),DIMEN(I,J5),DIMEN(I,J6))
    READ (51,401) (DIMEN(I,J7),DIMEN(I,J8),DIMEN(I,J9),
!DIMEN(I,J10),DIMEN(I,J11),DIMEN(I,J12))
    READ (54,401) (DIMEN(I,J13),DUMP,DUMP,DUMP,DIMEN(I,J14),
!AUTH(I))
401   FORMAT (6E10.3)
22    CONTINUE
    IF (J14.EQ.15) GO TO 1
    ENDALL = ENDEXP
    GO TO 2
1     BGNLIT=ENDEXP+1
    ENDALL=ENDEXP+ENDLIT
    DO 26 I=BGNLIT,ENDALL
    IF (L1.EQ.1) GO TO 25
    READ (45,402) DIMEN(I,K1),DIMEN(I,K2),DIMEN(I,K3),
!DIMEN(I,K4),DIMEN(I,K5),DIMEN(I,K6),DIMEN(I,K7),
!DIMEN(I,K8),DIMEN(I,K9),DIMEN(I,K10),DIMEN(I,K11),
!DIMEN(I,K12),DIMEN(I,K13),DIMEN(I,K14)
25    READ (30,403) (DIMEN(I,J1),DIMEN(I,J2),DIMEN(I,J3),DIMEN(
!I,J4),DIMEN(I,J5),DIMEN(I,J6),DIMEN(I,J7))
    READ (32,403) (DIMEN(I,J8),DIMEN(I,J9),DIMEN(I,J10),DIMEN
!(I,J11),DIMEN(I,J12),DIMEN(I,J13),AUTH(I))
403   FORMAT (7E10.3)
26    CONTINUE
2     I1=0
    DO 5 I=1,ENDALL
    PROD=1.
    DO 3 J=1,NOVAR
    PROD=PROD*DIMENT(I,J)
3     IF (PROD.LE.0.) GO TO 4
    I1=I1+1
    AUTH(I1)=AUTH(I)
    GO TO 5
4     DO 5 J=1,NOVAR
    DIMENT(I,J)=0.

```

```

5    CONTINUE
J0=0
I1=0
DO 7 J=1,NOVAR
IF (J.EQ.DEPEN) GO TO 6
J0=J0+1
ISAVE(J0)=J
6    DO 7 I=1,ENDALL
IF (DIMEN(I,J).EQ.0.) GO TO 7
I1=I1+1
X(I1)=ALOG(DIMEN(I,J))
7    CONTINUE
N=I1/NOVAR
CALL CORRE(N,NOVAR,1,X,XBAR,STD,RX,R,D,B,T)
NOVAR1=NOVAR-1
CALL ORDER(NOVAR,R,DEPEN,NOVAR1,ISAVE,RX,RY)
CALL MINV(RX,NOVAR1,DET,B,T)
CALL MULTRN(N,NOVAR1,XBAR,STD,D,RX,RY,ISAVE,B,SB,T,ANS)
TYPE 905, NOVAR,N
905  FORMAT(' MULTIPLE LINEAR REGRESSION: ',I2,' VARIABLES ',
!I4,' OBSERVATIONS.')
TYPE 906
906  FORMAT(//'* REGRESSION COEFFICIENTS: ')
TYPE 907,(ISAVE(I),B(I),I=1,NOVAR1)
907  FORMAT(IX,I10,G15.5)
TYPE 908
908  FORMAT(//'* STANDARD DEVIATION OF REGRESSION COEFFICIENTS: ')
TYPE 909,(ISAVE(I),SB(I),I=1,NOVAR1)
909  FORMAT(IX,I10,G15.5)
TYPE 910
910  FORMAT(//'* T VALUES: ')
TYPE 911,(ISAVE(I),T(I),I=1,NOVAR1)
911  FORMAT(IX,I10,G15.5)
TYPE 912,(ANS(I),I=1,10)
912  FORMAT(//'* INTERCEPT: ',G12.5,
1///' MULTIPLE CORRELATION COEFFICIENT: ',G12.5,
1///' STANDARD ERROR OF ESTIMATE: ',G12.5,
1///' SUM OF SQUARES ATTRIBUTED TO REGRESSION, SSAR: ',G12.5,
1///' DEGREES OF FREEDOM OF SSAR: ',G12.5,
1///' MEAN SQUARE OF SSAR: ',G12.5,
1///' SUM OF SQUARES OF DEVIATION FROM REGRESSION, SSDR: ',G12.5,
1///' DEGREES OF FREEDOM OF SSDR: ',G12.5
1///' MEAN SQUARE OF SSDR: ',G12.5,
1///' F VALUE: ',G12.5)
DO 9 I=1,N
FINAL(I,1)=EXP(ANS(I))
DO 8 K=1,NOVAR1
KK=(ISAVE(K)-1)*N+I
FINAL(I,1)=FINAL(I,1)*EXP(X(KK))**B(K)

```

```

8    CONTINUE
IDEPEN=I+(DEPEN-1)*N
FINAL(I,2)=EXP(X(IDEPE
9    CONTINUE
TYPE 913
913  FORMAT (//,28X,'DEPENDENT VARIABLE',//,
!4X,'CALCULATE EXPERIMENT      CALCULATE EXPERIMENT',
!4X,'CALCULATE EXPERIMENT',//)
TYPE 914, (FINAL(I,1),FINAL(I,2),I=1,N)
914  FORMAT (4X,2E10.3,4X,2E10.3,4X,2E10.3)
PAUSE 'IF A PLOT OF THESE RESULTS IS DESIRED, TYPE G<CR>,
!AND PLOT #<CR>. ELSE TYPE X<CR>.'
CALL DECWAR(FINAL,N)
CALL EXIT
END

```

### 8.3.3.2 DECWAR.

```

SUBROUTINE DECWAR(FINAL,N)
DIMENSION FINAL(1),A(8000)
ACCEPT *, JK
CALL PLOTS(A,5000)
CALL NUMBER(0.125,0.125,0.25,JK,0.0,'(13)',3)
CALL PLOT(1.5,1.5,3)
CALL PLOT(1.5,9.5,2)
CALL PLOT(9.5,9.5,1)
CALL PLOT(9.5,1.5,1)
CALL PLOT(1.5,1.5,1)
CALL PLOT(9.5,9.5,1)
CALL PLOT(1.5,1.5,3)
X1=1.5
Y1=1.5
DO 50 J=1,9
X1=X1+.8
50  CALL SYMBOL(X1,Y1,.125,13,0.0,-1)
CALL PLOT(1.5,1.5,3)
X1=1.5
DO 70 J=1,9
Y1=Y1+.8
70  CALL SYMBOL(X1,Y1,.125,15,0.0,-1)
DO 90 I=1,N
FINAL(I)=1.5+8.0*FINAL(I)
I1=2000+I
FINAL(I1)=1.5+8.0*FINAL(I1)
90  CALL SYMBOL(FINAL(I),FINAL(I1),.035,3,0.0,-1)
CALL PLOT(17.,0.,-3)
RETURN
END

```

8.3.3.3 DIMLES.

```

INTEGER UNIT,UNIT1,UNIT2,UNIT3
TYPE 50
50 FORMAT(IX,'FORM DIMENSIONLESS GROUPS',/IX,'ENTER
!# OF DATA POINTS')
ACCEPT *, NLines
TYPE 60
60 FORMAT(IX,'ENTER PROPER FILE NUMBERS',/IX,
! '48,51,54,33 FOR EXPERIMENTAL DATA',/IX,
! '30,32, 0,45 FOR LITERATURE DATA')
ACCEPT *, UNIT1,UNIT2,UNIT3,UNIT
OPEN (UNIT=UNIT,ACCESS='APPEND')
DO 4 I=1,NLines
IF (UNIT3.EQ.0) GO TO 2
READ (UNIT1,100) UG,UL,DP,RHOS,RHOL,RHOG
READ (UNIT2,100) SIGMA,VI SCOS,EPSS,EPSSM1,EPSG,EPSL
READ (UNIT3,100) DC
100 FORMAT (6E10.3)
GO TO 3
2 READ (UNIT1,101) UG,UL,DP,RHOS,RHOL,RHOG,SIGMA
READ (UNIT2,101) VI SCOS,EPSS,EPSSM1,EPSG,EPSL,DC
101 FORMAT (7E10.3)
3 REL=DP*UL*RHOL/VI SCOS
REG=DP*UG*RHOG/VI SCOS
WEL=RHOL*DP*UL**2/SIGMA
WEG=RHOG*DP*UG**2/SIGMA
FRL=UL**2/(980.*DP)
FRG=UG**2/(980.*DP)
BO=(RHOS-RHOL)*DP**2*980./SIGMA
AR=DP**3.*(RHOS-RHOL)*RHOL*980./VI SCOS**2
CA=VI SCOS*UL/SIGMA
CD=980.*(RHOS-RHOL)*DP/(RHOS*UL**2)
GA=980.*RHOS**2*DP**3/VI SCOS**2
UGUL=UG/UL
DCDP=DC/DP
ORNL=RHOL*UG**4./(980.*SIGMA)
WRITE (UNIT,102) WEL,WEG,FRG,FRL,REL,REG,UGUL,DCDP,
!GA,ORNL,BO,AR,CA,CD
102 FORMAT (14E10.3)
4 CONTINUE
CALL EXIT
END

```

8.3.4 Sample Program Execution

```
•EX CORRLT,LIBRARY,DECWAR,SYS: PLOT/SEA
FORTRAN: CORRLT
MAIN.
LINK:    LOADING

[LNKXCT CORRLT EXECUTION]
IF YOU WANT A LIST OF CORRELATION OPTIONS, TYPE 1 <CR>. ELSE TYPE 2 <CR>

1
TYPE 1 <CR> FOR DIMENSIONAL GROUPS ONLY
TYPE 2 <CR> FOR DIMENSIONLESS GROUPS ONLY
TYPE 3 <CR> FOR BOTH DIMENSIONAL AND NONDIMENSIONAL
2
TO CORRELATE EPSS : TYPE ITEM#. ELSE 15 <CR> #

15
TO CORRELATE 1-EPSS: TYPE ITEM#. ELSE 15 <CR> #
1
TO CORRELATE EPSG : TYPE ITEM#. ELSE 15 <CR> #
15
TO CORRELATE EPSL : TYPE ITEM#. ELSE 15 <CR> #
15
TO CORRELATE WEL : TYPE ITEM#. ELSE 15 <CR> #
15
TO CORRELATE WEG : TYPE ITEM#. ELSE 15 <CR> #
15
TO CORRELATE FRG : TYPE ITEM#. ELSE 15 <CR> #
15
TO CORRELATE FRL : TYPE ITEM#. ELSE 15 <CR> #
15
TO CORRELATE REL : TYPE ITEM#. ELSE 15 <CR> #
2
TO CORRELATE REG : TYPE ITEM#. ELSE 15 <CR> #
15
TO CORRELATE UG/UL : TYPE ITEM#. ELSE 15 <CR> #
15
TO CORRELATE DC/DP : TYPE ITEM#. ELSE 15 <CR> #
15
TO CORRELATE GA : TYPE ITEM#. ELSE 15 <CR> #
3
TO CORRELATE ORNL : TYPE ITEM#. ELSE 15 <CR> #
15
TO CORRELATE BO : TYPE ITEM#. ELSE 15 <CR> #
15
TO CORRELATE AR : TYPE ITEM#. ELSE 15 <CR> #
15
```

```
TO CORRELATE CA : TYPE ITEM#. ELSE 15 <CR> #
15
TO CORRELATE CD : TYPE ITEM#. ELSE 15 <CR> #
15
THE NUMBER OF VARIABLES CHOSEN =
3
THE ITEM NUMBER OF THE DEPENDENT VARIABLE =
1
THE NUMBER OF LINES OF EXPERIMENTAL INPUT =
334
THE NUMBER OF LINES OF LITERATURE INPUT =
1223
15 15 15 15 15 15 15 15 15 1 15 15 15 15 15 15 15 15 2 15 15 15 3 15
15 15 15 15 3 1 334 1223
```

MULTIPLE LINEAR REGRESSION: 3 VARIABLES 1475 OBSERVATIONS.

REGRESSION COEFFICIENTS:
2 0.27533
3 -0.17103

STANDARD DEVIATION OF REGRESSION COEFFICIENTS:
2 0.52558E-02
3 0.28738E-02

T VALUES:
2 52.387
3 -59.512

INTERCEPT: 0.42730

MULTIPLE CORRELATION COEFFICIENT: 0.84239
STANDARD ERROR OF ESTIMATE: 0.11048

SUM OF SQUARES ATTRIBUTED TO REGRESSION, SSAR: 43.910

DEGREES OF FREEDOM OF SSAR: 2.0000

MEAN SQUARE OF SSAR: 21.955
SUM OF SQUARES OF DEVIATION FROM REGRESSION, SSDR: 17.968

DEGREES OF FREEDOM OF SSDR: 1472.0

MEAN SQUARE OF SSDR: 0.12206E-01

F VALUE: 1798.7

## DEPENDENT VARIABLE

CALCULATE EXPERIMENT	CALCULATE EXPERIMENT	CALCULATE EXPERIMENT
0.393E+00 0.404E+00	0.418E+00 0.417E+00	0.440E+00 0.455E+00
0.459E+00 0.466E+00	0.476E+00 0.466E+00	0.492E+00 0.516E+00
0.506E+00 0.525E+00	0.393E+00 0.455E+00	0.418E+00 0.443E+00
0.440E+00 0.455E+00	0.459E+00 0.477E+00	0.476E+00 0.516E+00
0.492E+00 0.516E+00	0.506E+00 0.534E+00	0.365E+00 0.359E+00
0.393E+00 0.423E+00	0.418E+00 0.404E+00	0.440E+00 0.466E+00
0.459E+00 0.507E+00	0.476E+00 0.497E+00	0.492E+00 0.516E+00
0.365E+00 0.390E+00	0.393E+00 0.404E+00	0.418E+00 0.443E+00
0.440E+00 0.466E+00	0.459E+00 0.466E+00	0.476E+00 0.507E+00
0.492E+00 0.487E+00	0.506E+00 0.507E+00	0.449E+00 0.447E+00
0.477E+00 0.476E+00	0.502E+00 0.488E+00	0.524E+00 0.486E+00

IF A PLOT OF THESE RESULTS IS DESIRED, TYPE G<CR>, AND PLOT #<CR>. ELSE TYPE X<CR>.

TYPE G TO CONTINUE, X TO EXIT, T TO TRACE.

\*G

56

!SAVE THIS PLOT? Y FOR YES

Y

!SAVED PLOT 1

END OF EXECUTION

CPU TIME: 1:47.08

ELAPSED TIME: 11:8.80

EXIT

.Q PLT:=FOR29.DAT/DISP:RENAME

TOTAL OF 213 BLOCKS IN PLT REQUEST

### 8.4 Location of Data

The original data are located in ORNL Databooks A-7550-G, pp. 1-100, and A-6976-G, pp. 80-88. The databooks and calculations are on file at the MIT School of Chemical Engineering Practice, Bldg. 3001, ORNL.

### 8.5 Nomenclature

A	cross-sectional area of the column, $\text{cm}^2$
Ar	Archimedes number, $d_p^3 g (\rho_S - \rho_L) \rho_L / \mu_L^2$
a	correlation coefficient
b	correlation coefficient
c	correlation coefficient
D <sub>C</sub>	diameter of the column, cm
d <sub>p</sub>	diameter of the solid particles, cm
Fr	Froude number, $U_f^2 / gd$
Ga	Galileo number, $d_p^3 \rho_S^2 g / \mu_L^2$
g	gravitational constant, $\text{cm/sec}^2$
H	distance up the column, cm
H <sub>B</sub>	height of fluidized bed, cm
h	height of liquid in manometer, cm of fluid
M	mass, gm
n	number of independent experimental variables
p	pressure, dynes/cm <sup>2</sup>
q	general experimental variable
Δq	error involved in measurement of variable q
Re	Reynolds number, $\rho_f U_f d_p / \mu_f$
S	bed pressure gradient, cm fluid/cm
U	superficial fluid velocity, cm/sec

W weight, dynes

Greek Symbols

$\epsilon$  holdup, i.e., volume fraction of specific phase  
 $\rho$  density, gm/cm<sup>2</sup>  
 $\sigma$  surface tension, dyne/cm  
 $\mu$  viscosity, poise

Subscripts

B bed  
buoy buoyant  
G gas phase  
f fluid  
i ith phase or ith variable  
L liquid phase  
mf minimum fluidization  
p particle  
S solid phase

8.6 Literature References

1. Bhatia, V.K., and N. Epstein, "Three-Phase Fluidization: A Generalized Wake Model," Proc. of Intern. Symp. on Fluidization and Its Applications, Toulouse, October, 1973, Cepadues Editions.
2. Bruce, P.N., and L. Revel-Chion, "Bed Porosity in Three-Phase Fluidization," Powder Tech., 10, 243 (1974).
3. Burck, G.M., K. Kodama, R.G. Markeloff, and S.R. Wilson, "Cocurrent Three-Phase Fluidized Bed (Part 2)," ORNL/MIT-213 (May 1975).
4. Dakshinamurty, P., V. Subrahmanyam, and J.N. Rao, "Bed Porosities in Gas-Liquid Fluidization," I&EC Proc. Des. Dev., 10, 322 (1971).
5. Darton, R.C., and D. Harrison, "Gas and Liquid Holdup in Three-Phase Fluidization," Chem. Eng. Sci., 30, 581 (1975).

6. Efremov, G.I., and I.A. Vakhrushev, "A Study of the Hydrodynamics of Three-Phase Fluidized Beds," Intern. Chem. Eng., 10(1), 37 (1970).
7. Ferguson, D.E., ed., "Chemical Technology Division Annual Progress Report for the Period Ending March 31, 1974," ORNL-4966.
8. Khosrowshahi, S., S.R. Bloxom, C. Guzman, and R.M. Schlapfer, "Determination and Correlation of Hydrodynamic Variables in a Three-Phase Fluidized Bed," ORNL/MIT-216 (Sept. 1975).
9. Kim, S.D., C.G.J. Baker, and M.A. Bergougnou, "Phase Holdup Characteristics of Three-Phase Fluidized Beds," Can. J. Chem. Eng., 53, 134 (1975).
10. Kline, S., and F.A. McClintock, "Describing Uncertainties in Single-Sample Experiments," Mech. Eng., 75, 3 (1953).
11. Mukherjee, R.N., P. Bhattacharya, and D.K. Taraphdar, "Studies on the Dynamics of Three-Phase Fluidization," Proc. of the Intern. Symp. on Fluidization and Its Applications, Toulouse, October 1973, Cepadues Editions.
12. Østergaard, K., and M.L. Michelson, "Holdup and Axial Dispersion in Gas-Liquid Fluidized Beds," Preprint 31D, Symp. on Fundamental and Applied Fluidization, Tampa, May 1968.
13. Østergaard, K., and P.I. Theisen, "The Effect of Particle Size and Bed Height on the Expansion of Mixed Phase (Gas-Liquid) Fluidized Beds," Chem. Eng. Sci., 21, 413 (1966).
14. Rigby, G.R., and C.E. Capes, "Bed Expansion and Bubble Wakes in Three-Phase Fluidization," Can. J. Chem. Eng., 48, 343 (1970).
15. Wen, C.Y., and Y.H. Yu, "Mechanics of Fluidization," Chem. Eng. Progr. Symp. Series, 62, 100 (1966).

ORNL/MIT-219

INTERNAL DISTRIBUTION

1. J.M. Begovich
2. H.D. Cochran
3. C.W. Hancher
4. D.W. Holladay
5. J.M. Holmes
6. D.D. Lee
7. Yvonne Lovely
8. J.P. Nichols
9. G.D. Robbins
10. C.D. Scott
11. J.S. Watson
- 12-13. Central Research Library
14. Document Reference Section
- 15-17. Laboratory Records
18. Laboratory Records, ORNL R.C.
19. ORNL Patent Office
- 20-21. Technical Information Center
- 22-36. MIT Practice School

EXTERNAL DISTRIBUTION

37. C.O. Reiser, Arizona State U., Tempe
38. J.E. Vivian, MIT
39. Director, Research and Technical Support  
Division, ERDA-ORO